UNIVERSIDADE TECNOLÓGICA FEDERAL DO PARANÁ

MARA REGINA ALVES DE ASSIS

ANALYSIS OF INSULATING OIL IN POWER TRANSFORMERS USING LMR SENSORS

CURITIBA

2025

MARA REGINA ALVES DE ASSIS

ANALYSIS OF INSULATING OIL IN POWER TRANSFORMERS USING LMR SENSORS

ANÁLISE DE ÓLEO ISOLANTE DE TRANSFORMADOR DE POTÊNCIA UTILIZANDO SENSOR LMR

Master's Dissertation presented as a requirement to obtain the title of Master in Programa de Pós-Graduação em Sistemas de Energia (PPGSE) from Universidade Tecnológica Federal do Paraná (UTFPR).

Advisor: Prof. Dr.Uilian José Dreyer

Co-advisor: Prof. Dr.Jean Carlos Cardozo da Silva

Co-advisor: Prof. Dr. Carlos Ruiz Zamarreño

CURITIBA
2025

Ministério da Educação
Universidade Tecnológica Federal do Paraná
Campus Curitiba

MARA REGINA ALVES DE ASSIS

ANALYSIS OF INSULATING OIL IN POWER TRANSFORMERS USING LMR SENSORS

Trabalho de pesquisa de mestrado apresentado como requisito para obtenção do título de Mestre Em Engenharia Elétrica da Universidade Tecnológica Federal do Paraná (UTFPR). Área de concentração: Automação E Sistemas De Energia.

Data de aprovação: 24 de Novembro de 2025

Dr. Uilian Jose Dreyer, Doutorado - Universidade Tecnológica Federal do Paraná

Dr. Cleumar Da Silva Moreira, Doutorado - Instituto Federal de Educação, Ciência e Tecnologia do Paraná (Ifpr)

Dr. Gustavo Gomes Kuhn, Doutorado - Universidade Tecnológica Federal do Paraná

Documento gerado pelo Sistema Acadêmico da UTFPR a partir dos dados da Ata de Defesa em 24/11/2025.

I dedicate this work to my family.

ACKNOWLEDGEMENTS

First and foremost, I thank God for His infinite wisdom and for guiding my path throughout this journey.

I express my sincere gratitude to my advisor for his patience, generosity in sharing his knowledge and experiences, and for making this work possible.

To my husband, Luiz, and my son, Guilherme, I am grateful for their unconditional support and understanding during my periods of absence.

To my colleague Matheus Camargo, for his essential collaboration in the development of this research, and to all my colleagues at UTFPR and the laboratory technicians, for their valuable partnership, I express my gratitude.

I would like to express my special thanks to the funding agencies CAPES, CNPQ, FINEP, Araucária Foundation e SETI, as well as the Photonics Multi-user Facility-UTFPR- for institutional support.

"This project was funded by the National Council for Scientific and Technological Development (CNPq) through process no. 406145/2022-9."

‘Try to move the world, the first step will be to move yourself’ - Plato

RESUMO

ASSIS, Mara. **ANALYSIS OF INSULATING OIL IN POWER TRANSFORMERS USING LMR SENSORS**. 2025. 76 f. (Mestrado em Sistemas de Energia) – Universidade Tecnológica Federal do Paraná, Curitiba, 2025.

Os transformadores de potência isolados a óleo constituem elementos essenciais dos sistemas de energia elétrica. O sistema de isolamento destes equipamentos é formado pela combinação do óleo isolante e do papel kraft, que, além de garantir a rigidez dielétrica, contribui para a capacitância entre os enrolamentos. A fim de preservar a qualidade desse óleo, torna-se indispensável a realização periódica de análises físico-químicas. A ocorrência de falhas nesses transformadores pode acarretar derramamentos de óleo e incêndios, resultando em danos significativos aos sistemas interconectados. Nesse contexto, sensores de fibra óptica despontam como uma alternativa promissora, dada sua elevada sensibilidade, seletividade e curto tempo de resposta. Este trabalho investiga a aplicação de sensores ópticos baseados em ressonância de modo com perdas (Lossy Mode Resonance – LMR), fabricados a partir de fibras ópticas com a casca removida e recobertas por filmes finos de óxido metálico — especificamente óxido de zinco (ZnO) — como ferramenta para detecção e monitoramento da qualidade do óleo isolante em transformadores de potência. O princípio de funcionamento do sensor LMR associa a variação do comprimento de onda (λ) e o do índice de refração (n) a parâmetros relacionados ao nível de degradação do óleo isolante. O arranjo experimental foi constituído por uma fonte de luz branca modelo AQ4305 (Yokogawa) e por um espectrômetro Ocean Optics QE65000, possibilitando a calibração do sensor com sensibilidade da ordem de 345,78 nm/RIU. Para a realização das análises, foram utilizadas quatro amostras de óleo submetidas a ciclos térmicos variando entre 25 °C e 60 °C. Os resultados obtidos evidenciaram deslocamentos espectrais na região correspondente à faixa espectral da cor azul. Observou-se, contudo, que o comportamento espectral diferiu entre as amostras quando expostas às variações de temperatura: as amostras novas ou pouco degradadas apresentaram maior sensibilidade óptica, manifestando deslocamentos mais pronunciados, enquanto as amostras mais degradadas exibiram variações espectrais reduzidas. Esse comportamento foi atribuído às propriedades físico-químicas dos óleos , tais como índice de refração, densidade, rigidez dielétrica e presença de água e gases. Tais propriedades apresentaram correlação direta com os resultados das análises laboratoriais. Os achados demonstraram a eficácia da técnica LMR na detecção de alterações físico-químicas em óleos isolantes, destacando seu potencial para o monitoramento em tempo real do processo de envelhecimento desses materiais. Tal monitoramento é de relevância fundamental para assegurar a integridade e a confiabilidade operacional dos transformadores de potência.

Palavras-chave: Óleo isolante, Transformadores, Sensor LMR.

ABSTRACT

ASSIS, Mara. **ANÁLISE DE ÓLEO ISOLANTE DE TRANSFORMADOR DE POTÊNCIA UTILIZANDO SENSOR LMR**. 2025. 76 f. (Mestrado em Sistemas de Energia) – Universidade Tecnológica Federal do Paraná, Curitiba, 2025. Título original: ANALYSIS OF INSULATING OIL IN POWER TRANSFORMERS USING LMR SENSORS

Oil-insulated power transformers are essential components of electrical power systems. The insulation system of this equipment consists of a combination of insulating oil and kraft paper, which, in addition to ensuring dielectric strength, contributes to the capacitance between the windings. To preserve the quality of this oil, it is essential to perform periodic physical-chemical analyses. Failures in these transformers can lead to oil spills and fires, resulting in significant damage to interconnected systems. In this context, fiber optic sensors are emerging as a promising alternative, given their high sensitivity, selectivity, and short response time. This work investigates the application of optical sensors based on lossy mode resonance (LMR), manufactured from optical fibers with the cladding removed and covered with thin films of metal oxide — specifically zinc oxide (ZnO)—as a tool for detecting and monitoring the quality of insulating oil in power transformers. The operating principle of the LMR sensor associates the variation in wavelength (λ) and refractive index (n) with parameters related to the level of degradation of the insulating oil. The experimental setup consisted of an AQ4305 white light source (Yokogawa) and an Ocean Optics QE65000 spectrometer, enabling sensor calibration with a sensitivity of approximately 345.78 nm/RIU. Four oil samples submitted to thermal cycles ranging from 25 °C to 60 °C were used to perform the analyses. The results obtained showed spectral shifts in the region corresponding to the blue spectral range. However, it was observed that the spectral behavior differed between samples when exposed to temperature variations: new or slightly degraded samples showed greater optical sensitivity, manifesting more pronounced shifts, while the more degraded samples exhibited reduced spectral variations.This behavior was attributed to the physical and chemical properties of the oils, such as refractive index, density, dielectric strength, and the presence of water and gases. These properties were directly correlated with the results of laboratory analyses. The findings demonstrated the effectiveness of the LMR technique in detecting physical-chemical changes in insulating oils, highlighting its potential for real-time monitoring of the aging process of these materials. Such monitoring is of fundamental importance to ensure the integrity and operational reliability of power transformers.

Keywords: Insulating Oil, Transformers, LMR Sensor.

LIST OF FIGURES

LIST OF TABLES

LIST OF ABBREVIATIONS

CAPES	Coordenação de Aperfeiçoamento de Pessoal de Nível Superior
CNPQ	Conselho Nacional de Desenvolvimento Científico e Tecnológico
FINEP	Financiadora de Estudos e Projetos
SETI	Superintendência Geral de Ciência, Tecnologia e Ensino Superior
UTFPR	Universidade Tecnológica Federal do Paraná
LMR	Lossy Mode Resonance
GW	Gigawatts
DGA	Dissolved Gas Analysis
AC	Alternating Current
HVDC	High Voltage Direct Current
DP	Degree of Polymerization
DF	Dissipation Factor
PF	Power Factor
RVM	Voltage Recovery Method
PDC	Polarization/Depolarization Currents
FDS	Frequency Domain Spectroscopy
SFRA	Sweep Frequency Response Analysis
RI	Refractive Index
DGA	Dissolved Gas Analysis
LPGS	Optical fibers Based on Long Period Networks
QE65000	Ocean Optics Spectrometer
AQ4305	White Light Source Yokogawa

LIST OF SYMBOLS

λ	wavelength
n	refractive index
ε'	Real Part of Material Permittivity
ε_r	Relative Permittivity of the Material
ε''	Imaginary Part of Permittivity
$\mathbf{E}$	Electric Field
$\mathbf{B}$	Magnetic Field
λm	Average Wavelength

CONTENTS

1 INTRODUCTION

In the first half of 2024, Brazil's electricity grid expanded by approximately 6.4 GW. This increase in capacity is due to the commissioning of 10 photovoltaic solar plants and 17 wind farms. The expansion of renewable energy sources is a key factor in the country's energy transition (Agência Nacional de Energia Elétrica, 2024).

The rapid increase in power generation, added to the already installed capacity, increases the need for electrical grid infrastructure. In this system, electrical power transformers installed in substations and power plants are essential components. A power transformer is an electrical device that changes the input voltage and current levels to different output magnitudes, according to the specifications of the system in which it is installed. A key component of the power transformer is mineral oil. This oil has thermal and temporal stability, in addition to offering excellent electrical insulation properties. It also acts as a temperature regulator within the transformer, as well as being an integral part of the electrical insulation between the active internal components. For this reason, the oil needs to be monitored regularly to ensure that its quality is acceptable and maintains the integrity of the power transformer. (FIGUEIREDO; MARTINS-FILHO, 2005).

The failure of a power transformer results not only in downtime for the transmission and distribution network, but also in personal and environmental risks due to oil leaks and fires. To increase reliability and extend the service life of transformers, it is necessary to adopt a reliable and cost-effective monitoring technique from the moment of installation. This approach allows for early detection of failures and extends the operational life of the equipment. Systematic monitoring of the condition of mineral insulating oil through routine testing and diagnostics is intended to monitor equipment conditions and assess the aging and defects of the core, windings, bushings, and tap changers of power transformers. (ISLAM LEE; HETTIWATTE, 2018). To improve service quality and reduce the operating cost of an operating transformer, different condition monitoring and diagnostic techniques are currently in use. Short-circuit and overload faults increase the likelihood of unexpected failures throughout the electrical power system. Over the years, a wide variety of sensor technologies that can be used for fault diagnosis methods **online** or **offline** were developed for power transformer monitoring systems (JIN et al., 2022).

Online condition monitoring has been widely used in the maintenance of power equipment in various fields. Although promising, this approach faces practical problems such as low data availability and reliability. In addition, there is a significant lack of international standards for online monitoring, highlighting the urgent need to establish such standards (GUO;

DONG, 2019).

This study proposes a method for monitoring oil quality and aging offline. Optical sensors based on Loss Mode Resonance (LMR) have been investigated as a viable alternative for monitoring physical parameters in electrical systems, standing out for their sensitivity and electromagnetic immunity. Such characteristics inherent to fiber optic detection devices, such as low weight, small size, wavelength measurements, and electromagnetic immunity, meet all these requirements. (MEITEI; BORAH, 2023).

1.1 MOTIVATION

Understanding the operating conditions of power transformers installed in substations of the national interconnected system is undoubtedly essential for the reliability and efficiency of the electricity sector. On a global scale, continuous monitoring of this equipment is a well-established and strategic practice, since transformers are critical elements in the transmission and distribution of electrical energy. Failures in these devices can cause significant interruptions in supply, resulting in economic losses, impacts on the stability of the electrical system, and risks to operational safety. For energy utilities, the adoption of effective monitoring systems is essential to improve investment planning and optimize maintenance and replacement decisions, promoting greater availability and longevity of equipment. In this context, this study proposes the use of optical sensors as a technology to support the evaluation of the condition of insulating oil in power transformers, given the importance of this equipment in high-voltage substations. The choice of optical sensors over other monitoring technologies is justified by their superior characteristics of sensitivity, immunity to electromagnetic interference, rapid response, and ability to operate in harsh environments. In addition, optical sensors allow non-invasive and high-precision measurements, enabling early detection of changes in the physical and chemical properties of insulating oil—a direct indicator of the state of degradation of the transformer. Thus, a monitoring system based on this technology offers ample possibilities for optimizing operation, increasing the reliability of the electrical system, and contributing to the prevention of failures in power substations, which are among the main causes of interruptions in supply to consumers.

The graph in Figure 1 shows the compensation amounts paid individually. (Agência Nacional de Energia Elétrica, 2024).

Failures in power substations are largely responsible for interruptions in supply to consumers. ANEEL released a report on the amount of continuity compensation paid to consumers served by the distribution system during the year 2023. This amount is automatically

Figura 1 – Amount of Financial Compensation paid by Distributors

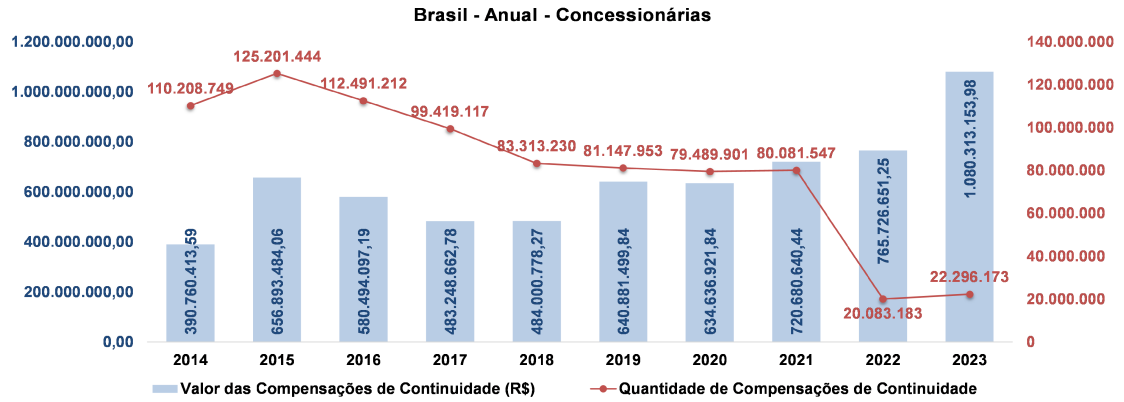

Source: (Agência Nacional de Energia Elétrica, 2024)

paid by the distributor, through a discount on the electricity bill, when a disruption in the supply of energy to consumers is detected, without the consumer having to contact the distributor to obtain reimbursement. Between 2021 and 2022, according to ANEEL data, there was a significant reduction in the number of continuity compensations, which fell from approximately 80 million to 20 million. However, the total amount paid increased from R$ 720 million in 2021 to approximately R$ 1.08 billion in 2023. The main reason for this change is that the agency implemented regulatory changes to give more weight to the principle of equity, which prioritizes consumers most affected by supply failures, rather than distributing large amounts of compensation to all consumers. This resulted in fewer compensations, a drop of approximately 60 million consumers, but each compensation became larger, about four times greater per affected consumer.

In the case of transformers, oil acts as an insulator, preventing short circuits between the different conductive parts of the transformer. In addition, oil helps dissipate the heat generated during transformer operation, preventing overheating. (MEITEI; BORAH, 2023).The analysis of physical-chemical parameters—such as density, dielectric strength, water content, among others—together with the analysis of dissolved gases (DGA) is a fundamental step in diagnosing incipient faults in transformer insulation systems. This approach allows the identification of gases and particles dissolved in insulating oil, which serve as indicators of internal faults, including degradation of the insulating material, as well as mechanical or electrical anomalies. Additionally, this procedure enables the assessment of characteristics associated with the useful life of the equipment, representing an indicator of the risk of failure and its systemic importance, reflecting the impact on the overall performance of the electrical system. Continuous monitoring of the condition of insulating oil also enables the planning of maintenance actions based on the actual operating condition of the equipment, which contributes to increased reliability, extended service life, and guaranteed operational safety

of these assets.(FRIEDENBERG; SANTANA, 2014).

1.2 OBJECTIVES

1.2.1 General Objective

The overall objective of this work is to develop a method for monitoring the condition of power transformer oil using an LMR optical sensor coated with a metallic zinc oxide (ZnO) film for this analysis.

1.2.2 Specific Objectives

- Conduct a literature review on the topic.
- Evaluate the performance and behavior of LMR sensors in terms of the calibration curve generated and the sensitivity determined, i.e., obtain the metrological characteristics for this device;
- Determine whether there is a correlation between the values measured by the LMR sensor and the values obtained in conventional oil analysis tests, such as chromatography and other physical-chemical tests.
- Collect measured data from transformer oil samples at various levels of degradation and establish a correlation with standard oil analysis methods.
- Analyze the different types of spectra obtained with and without temperature variation.
- Evaluate the functionality of the device for the required application.

1.3 CONTRIBUTIONS OF THIS RESEARCH PAPER

- Verification of the methodology for characterizing and calibrating LMR-type optical sensors for industrial applications, as a lower-cost alternative to commercially available sensors, and correlation with chromatography tests for monitoring the aging of insulating oil.
- Characterization of the refractive index of insulating oil in power transformers using LMR optical sensors as refractometers.
- To show an analysis of the determining factors of the conditions that indicate the degradation of transformer insulating oil and relate the refractive index of insulating oils

to other aspects of insulating oil samples, such as density and water content, present in oils collected from new equipment or equipment that has been in operation for long periods, allowing the characterization and classification of the oil conditions in this equipment.

- To show a correlation between the state of degradation of insulating oil and the occurrence of electrical faults in equipment.

Such contributions are fundamental to advancing knowledge in the field of research and application of LMR-type optical sensors and their possible industrial applications.

1.4 STRUCTURE AND ORGANIZATION OF THIS WORK

This dissertation is organized to provide the necessary theoretical foundation (Chapters 1 to 3), detail the experimental methodology (Chapters 4 and 5), and finally present and discuss the results obtained from the tests on insulating oil (Chapter 6), culminating in conclusions and future perspectives (Chapter 7).

Description of the Dissertation Structure by Chapters

- Chapter 1: Introduction - This chapter establishes the context of the research, addressing the relevance of oil-insulated power transformers in electrical power systems and the criticality of monitoring their quality. It presents the motivation for the study, which includes the need for reliable and economically viable monitoring techniques to extend the useful life of equipment and reduce the risk of catastrophic failures. This chapter defines the general objective (to develop a method for monitoring oil condition using the LMR sensor with zinc oxide (ZnO) film) and the specific objectives of the work.
- Chapter 2: Literature Review - This chapter provides the theoretical framework. It details power transformers, emphasizing the role of insulating oil in electrical insulation and thermal dissipation. The main theoretical section addresses optical sensors based on Lossy Mode Resonance (LMR), defining concepts such as electrical permittivity, refractive index (RI), and the evanescent wave coupling mechanism. A crucial distinction is made between Surface Plasmon Resonance (SPR) and LMR, highlighting the advantages of LMR (no strict polarization dependence and multiple mode capability).
- Chapter 3: Related Work - This chapter explores the state of the art in optical sensing, focusing on fiber optic applications for monitoring insulating oil in transformers. It reviews techniques for monitoring temperature, partial discharges, and dissolved gas analysis (DGA) using optical fibers and structures such as LPGs (Long Period Arrays).

The chapter reinforces the emerging potential of LMR technology in relation to SPR, especially due to its robustness and versatility in harsh environments.

- Chapter 4: Characterization and Calibration of the LMR Sensor This chapter describes the methodology and experimental setup used. It details the materials and equipment used, including the QE65000 Spectrometer, the AQ4305 White Light Source, and the Python code developed for spectral data processing. This chapter also presents the results of the initial calibration of the sensor, demonstrating the calibration curve obtained with water/glycerin solutions. It is in this chapter that the sensitivity of the LMR sensor is determined, which was 345.78 nm/RIU, and the importance of wavelength variation in the spectrum is explained.

- Chapter 5 - Calibration of the LMR Sensor with Temperature Variation and Tests with Insulating Oil - This chapter applies the LMR sensor under conditions of temperature variation (25 °C to 60 °C). The results of the tests with the four real samples of insulating oil (A, B, C, and D) are presented, detailing the spectral shift ($\Delta\lambda$) for each one. The integrated discussion of the results correlates the optical behavior (lower spectral shift in degraded oils) with the physical-chemical properties obtained in laboratory reports (dielectric strength, water content, and dissolved gases).

- Chapter 6: Conclusion - This chapter summarizes the main findings, confirming the effectiveness of the LMR technique in detecting physical-chemical changes in insulating oils. The study concludes that the LMR sensor is a flexible and versatile approach with potential for real-time monitoring.

2 LITERATURE REVIEW

This chapter will detail the characteristics and types of fault monitoring for power transformers used in both power distribution and transmission systems. In this regard, emphasis will be placed on the importance of insulating fluid in the performance of this equipment. In addition, a literature review on optical sensors based on lossy mode resonance will be discussed, highlighting their application as refractometers and as devices capable of detecting the aging of insulating oils through spectral analysis, since the LMR (Lossy Mode Resonance) sensor generates a resonance spectrum that can be analyzed to identify the interaction of the wavelength of the medium, for example, insulating oil, allowing the determination of the refractive index

2.1 POWER TRANSFORMER

Power transformers are essential devices for the transmission of electrical energy, allowing the transformation of voltages and currents in alternating current circuits and the modification of impedance values. For safety reasons, energy is delivered to consumers at low voltage levels (220/127 V). (ABNT, 2007).

Figura 2 – Electrical Power System

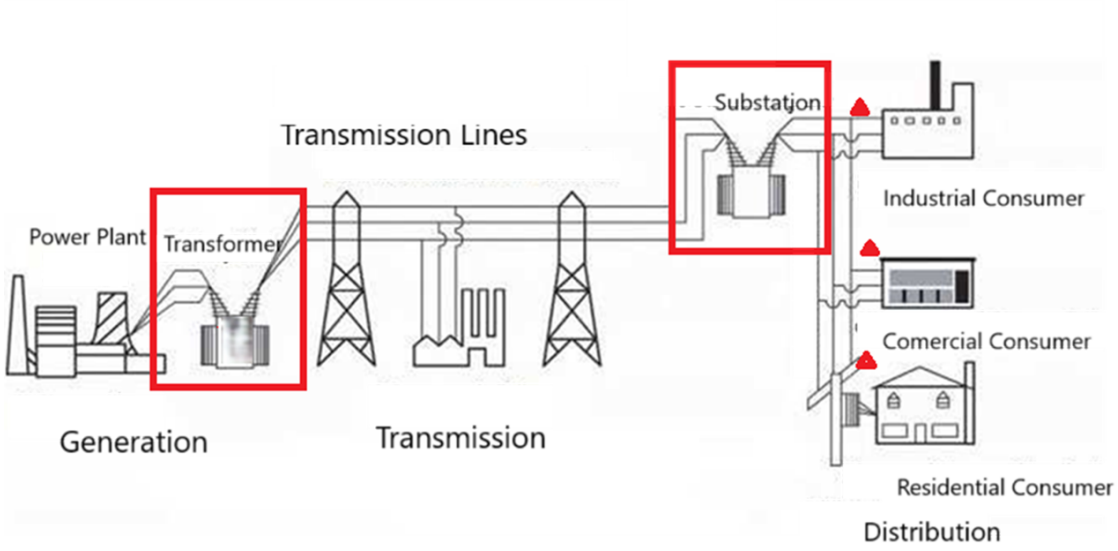

Source: Adapted from (MATTEDE, 2025)

Although the synchronous generator operates at medium voltage, the energy generated is not transmitted directly in this range. Immediately after generation, the voltage is raised by step-up transformers to high or extra-high voltage levels, suitable for transmitting electrical energy over long distances. Typical levels after this increase range from 69 kV to 138 kV for

subtransmission and regional interconnections, 230 kV to 500 kV for main transmission in large systems, and above 750 kV for alternating current transmission systems (AC) ultra-high voltage or direct current (HVDC) (GUO; DONG, 2019).

2.1.1 Power Transformer Oil Condition Analysis

Insulating oil performs electrical insulation and thermal dissipation functions in transformers. Therefore, proper maintenance of the condition of the insulating oil throughout the operational life of the transformer is essential to ensure reliable operation and extend the service life of the equipment. The condition of insulating oil is monitored by analyzing various physical, chemical, and electrical properties. The evaluation of gases dissolved in the oil is also extremely important in insulating oil analysis. The main parameters for monitoring insulating oil include:

- Concentration of dissolved water;
- Density;
- Dielectric strength;
- Acidity (neutralization number);
- Interfacial Tension;
- Dissipation Factor (at 20°C or 25°C and at 90°C or at 100°C);
- Color;
- Furan concentration (liquid chromatography);
- Dissolved Gas Analysis (DGA, gas chromatography);

Monitoring the quality of insulating oil is a common practice for assessing the condition of transformers in operation, since the condition of the oil directly influences the performance and service life of the transformer. Controlling the condition of the oil has proven to be effective, since over time, due to oxidation, chemical reactions, and various stresses (thermal, electrical, and chemical), the characteristics of the oil change (FRIEDENBERG; SANTANA, 2014). Physical, chemical, and electrical tests, such as dielectric breakdown voltage (DBV), power factor, interfacial tension (IFT), acidity, viscosity, color, and flash point, are performed to quantify these changes and diagnose the severity of the failures (ISLAM LEE; HETTIWATTE, 2018). DBV evaluates the strength of oil to withstand electrical stress, while the power factor test measures dielectric losses in oil (JIN et al., 2022). During service, acids, oxidation products,

moisture, and solid contaminants degrade the oil, and acidity testing is essential to assess this condition. IFT measures the attraction between oil and water molecules, helping to estimate contaminants and degradation products. Viscosity, color, and flash point tests are used to detect contaminants in aged oil. Correlated results are used to assess the condition of transformers and plan maintenance to prevent premature failures and costly interruptions (AZIS et al., 2012).

As for dissolved gas analysis (DGA), it should be noted that during the first two years of operation, new equipment shows higher monthly growth rates of combustible gases (MGR) compared to similar equipment that has been in operation for more than two years. After this period, these rates become more compatible with the data predicted in the dissolved gas testing standards. This aspect should be considered when performing chromatographic analyses of equipment from the same family, generating limit values and graphs of the evolution of combustible gas concentrations. Equipment that has been degassed or had its oil replaced with degassed oil has dissolved gas profiles similar to those of new equipment, requiring more frequent resampling in the first 12 months. Less frequent chromatographic sampling is also recommended in cases of overload, power surges, short circuits, warranty periods, suspected internal problems, or other specific conditions (ABNT, 2012).

Tabela 1 – Gas Formation in Oil and Correlation with Types of Failures

Gas Type	Failure
Carbon dioxide (CO_2)	Thermal decomposition
Carbon monoxide (CO)	Thermal or electrical faults (short circuits)
Hydrocarbons (C_2H_4, C_2H_6)	Thermal decomposition overheating
Nitrogen (N_2)	Thermal decomposition or atmospheric contamination.
Nitrogen oxides (NOx)	Electrical faults and overheating

Source: (ABNT, 2012)

According to standard (ABNT, 2012), the main gases formed in the insulating oil of power transformers are classified according to Table 1, and their correlation with different types of faults is essential for diagnosing internal anomalies. The presence of carbon dioxide (CO_2) and carbon monoxide (CO) is associated with the thermal degradation of insulating paper (cellulose), overheating of solid parts of the transformer, and natural aging of the insulating material. Hydrocarbons, on the other hand, indicate overheating of the insulating oil, with ethane normally related to moderate heating, while ethylene appears at higher temperatures, which may indicate the occurrence of partial arcs. The formation of nitrogen (N_2) and nitrogen oxides (NOx) is, in turn, linked to the presence of air in the system, which may indicate sealing failures or loss of integrity of the storage tank. In particular, nitrogen oxides (NOx) are associated with partial corona discharges in the presence of infiltrated air, while nitrogen (N_2), although it can be used intentionally in sealed transformers, when found in high and

unexpected concentrations, suggests unwanted air entering the system (IEC 60599, 2015).

2.1.2 Transformer Condition Monitoring Techniques

Traditionally, offline monitoring is performed during scheduled maintenance, offering high measurement accuracy but without enabling the detection of incipient faults in real time. In contrast, online monitoring has gained prominence with the increasing digitization of electrical substations, as it allows continuous monitoring of equipment operating conditions, reducing unplanned downtime and increasing operational safety. Despite technological advances, full integration between offline and online monitoring techniques still requires significant improvements in order to enable more accurate, comprehensive, and predictive diagnostics (ISLAM LEE; HETTIWATTE, 2018)

Offline monitoring comprises a set of laboratory and on-site methods designed to assess the integrity of transformer components. Among these methods, the analysis of the degree of polymerization stands out (DP), sed to assess the degradation of cellulose-based insulating paper, with new transformers having PD values between 1000 and 1400, while values below 250 indicate the end of service life. Its main limitation is the need for direct sampling of the material, which makes it unfeasible for use in transformers in operation. The analysis of furan compounds is another effective method for diagnosing the aging of cellulose insulation, based on the measurement of 2-furaldehyde (2-FAL) concentration. Currently, new approaches combining Ultraviolet Visible (UV-Vis) spectroscopy with artificial intelligence techniques are being developed, providing faster and lower-cost estimates. Interfacial tension and oil acidity are parameters used to assess the degradation of insulating oil by measuring oxidation products, although this method requires sophisticated laboratory equipment and specialized personnel. The dielectric breakdown voltage of the oil determines the insulating fluid's ability to withstand electrical stresses, with values below 30 kV indicating significant degradation. The insulation resistance test, in turn, measures the dielectric strength of the windings and insulation, with historical analysis of the results being essential for proper interpretation of degradation. Finally, the dissipation factor (DF) and the power factor (PF) are used to assess the condition of bushings and insulation systems, where PF values above 1% indicate degradation; it should be noted that there are already versions of these tests adapted for continuous online monitoring of bushings. Dielectric response methods are fundamental tools for assessing the electrical and mechanical conditions of power transformers, allowing for the accurate identification of degradation processes in the insulation system and internal structural failures. Among these methods, the Voltage Recovery Method stands out.(RVM), used to detect moisture in the insulation system by analyzing dielectric polarization and depolarization behavior; Polarization/Depolarization Currents (PDC), which allows separate evaluation of

the insulating role and the oil, providing additional information on the dielectric condition of the materials; and Frequency Domain Spectroscopy, which allows separate evaluation of the insulating role and the oil, providing additional information on the dielectric condition of the materials (PDC), which allows separate evaluation of the insulating paper and oil, providing complementary information on the dielectric condition of the materials; and Frequency Domain Spectroscopy (FDS), notable for its consistency of results and low sensitivity to external noise, widely used in field measurements. Another widely used method is Sweep Frequency Response Analysis (SFRA), which evaluates the mechanical integrity of windings by comparing frequency response curves obtained under different operating conditions; despite its high effectiveness in detecting displacements, deformations, and short circuits between turns, this test requires the transformer to be shut down during its execution. Finally, the Transformer Turns Ratio Test (TTR) is used to identify insulation faults between turns, core, and windings. It is essential for transformers operating in parallel, where the exact correspondence of the turns ratio is indispensable for load balancing and safe system performance. These methods are widely described and recommended in standards and specialized technical publications, such as (CIGRÉ Working Group A2, 2015), which reinforce their relevance in advanced diagnostics and predictive maintenance of power transformers.

2.2 THEORY ON OPTICAL SENSORS BASED ON LOSSY MODE RESONANCE (LMR)

A fiber optic-based LMR (Lossy Mode Resonance) sensor is developed from a fiber —usually multimode — whose cladding is removed in a specific region, exposing the core that acts as a waveguide. A thin film of sensitive material, such as metal oxides, zinc oxide (ZnO), titanium dioxide (TiO_2), tin dioxide (SnO_2), or indium tin oxide (ITO), using techniques such as sputtering deposition (ZUBIATE et al., 2016). For resonance to occur, the coating must have suitable optical properties that enable the evanescent wave of the fiber to couple with the lossy modes guided in the film. The fundamental condition for the existence of LMR is related to the complex permittivity of the material, which we will discuss in section 2.3. This relationship characterizes the film as a lossy dielectric material, allowing partial confinement of optical energy in the coating and the consequent generation of resonance. In addition, the refractive index of the thin film must be higher than the refractive index of the surrounding medium and substrate to sustain the lossy modes (see section 2.5).

2.3 ELECTRICAL PERMITTIVITY

According to the definition in (PORTO EDITORA, 2025), complex permittivity is a physical quantity that describes the response of a material to an oscillating electric

field, simultaneously considering the storage of electrical energy and the dissipative losses associated with the conduction or absorption of electromagnetic energy. In optics, the **electric permittivity** (ε) is also called the dielectric constant and is usually represented as a complex number:

$$\tilde{\varepsilon} = \varepsilon' + j\varepsilon'' \tag{1}$$

whence:

- ε' **(Real Part of Material Permittivity)**: The real part of permittivity is associated with the material's ability to polarize under the action of an applied electric field, which determines the amount of electrostatic energy stored in the medium. In physical terms, ε' expresses the dielectric behavior of the material, reflecting how the bound charges (electric dipoles) respond elastically to the field. Furthermore, ε' is directly linked to the **refractive index** of the material, since:

$$n^2 \approx \varepsilon_r \tag{2}$$

whence ε_r is the relative permittivity of the material. A positive real part is characteristic of dielectric materials, indicating that they can support the propagation of electromagnetic waves.

- ε'' **(Imaginary Part of Permittivity)**: This component represents the dissipation of electromagnetic energy within the material and is associated with mechanisms of energy absorption or gain. Values of $\varepsilon'' > 0$ indicate that the electromagnetic wave loses energy as it propagates—this energy is converted into heat or other forms of loss, resulting in optical signal attenuation.

According to (KO et al., 2022), passive materials are substances that do not generate energy but interact with electric, magnetic, or optical fields, influencing the propagation of signals and waves. Unlike active materials—such as semiconductors or amplifying devices—passive materials only respond to external stimuli in a predictable and controlled manner, without altering the system's energy balance. Optical fibers are typically composed of glass (silica) or dielectric polymers, materials that do not generate energy, amplify signals, or actively alter the light they carry—they merely guide it. This light-guiding function occurs due to the difference in refractive index between the core and the cladding, which causes light to propagate by total internal reflection. In the context of passive optical sensors, such as those based on loss mode resonance (LMR), the imaginary part of the permittivity plays a fundamental role, as it determines the level of coupling between the guided light and the

dissipative modes of the sensitive material. Thus, variations in ε'' , caused by environmental changes (such as refractive index, temperature, or chemical composition of the medium) alter the intensity and spectral position of the LMR resonance, enabling highly sensitive optical detection.

2.4 EVANESCENT FIELDS

As described by Saleh and Teich (SALEH; TEICH, 2007), the properties of evanescent waves, evanescent fields are electromagnetic fields that extend beyond the surface of a dielectric medium but decay exponentially with distance from the surface. They are generated when light propagates through a medium with a different refractive index. In optical sensors based on loss mode resonance (LMR), evanescent fields are used to excite resonance modes that are sensitive to the properties of the surrounding medium. Van der Waals theory is relevant here because Van der Waals forces can influence the interaction between evanescent fields and molecules in the medium, affecting the efficiency and sensitivity of the optical sensor based on loss modes (LMR)(ZUBIATE et al., 2016).

2.5 FUNDAMENTALS OF REFRACTIVE INDEX

The refractive index (n) arises from molecular polarizability and is described by the Lorentz-Lorenz formula.

The force exerted on a charged particle q moving quickly $\mathbf{v}$ in an electric field $\mathbf{E}$ and magnetic $\mathbf{B}$ (SI units) it is

$$\mathbf{F} = q\left(\mathbf{E} + \mathbf{v} \times \mathbf{B}\right). \tag{3}$$

The instantaneous power transferred to the particle is

$$P \equiv \mathbf{F} \cdot \mathbf{v} = q\mathbf{E} \cdot \mathbf{v}, \tag{4}$$

since $\mathbf{v} \cdot (\mathbf{v} \times \mathbf{B}) = 0$.

In relativistic terms, the equation of motion can be written as

$$\frac{d}{dt}(\gamma m\,\mathbf{v}) = q\left(\mathbf{E} + \mathbf{v} \times \mathbf{B}\right), \qquad \gamma = \frac{1}{\sqrt{1 - \frac{v^2}{c^2}}}. \tag{5}$$

Molecular density generally decreases with increasing temperature (due to thermal expansion), which tends to decrease the refractive index. On the other hand, polarizability generally increases with temperature, which tends to increase the refractive index. Polarizability

refers to the tendency of matter, when subjected to an electric field, to acquire an electric dipole moment in proportion to that applied field. It is a property of all matter, since matter is composed of elementary particles that have an electric charge, namely protons and electrons.

Materials with high thermal expansion (such as alkali halides and thallium) tend to have negative thermo-optic coefficients, while materials with low thermal expansion (such as diamond and silicon carbide) tend to have positive thermo-optic coefficients.

The study (TROPF et al., 1998) discusses the dependence of the refractive index on temperature. This explanation lies in the fact that as the temperature increases, the density of the material decreases (thermal expansion effect). Materials with high thermal expansion (such as alkali halides and thallium) tend to have negative thermo-optic coefficients, while materials with low thermal expansion (such as diamond and silicon carbide) tend to have positive thermo-optic coefficients. This reduction in density tends to reduce the refractive index, as there is less mass per volume to interact with light. Simultaneously, the increase in polarizability also affects the index, but the predominant effect is usually the decrease caused by thermal expansion. Although not specific to insulating oils, this behavior is consistent with liquids in general. The refractive index of liquids (such as oil, water, or alcohol) decreases linearly with increasing temperature, aligning with the principle of thermal expansion. Studies on lubricating oils show that volume increases with temperature, and consequently, density decreases—which reinforces the physical mechanism behind the reduction in refractive index. The spectral position of the resonance in an LMR sensor is strongly dependent on the (actual) refractive index of the external medium and the characteristics of the thin film. In addition, the amount of evanescent power interacting with the sample is a critical parameter for sensitivity. Contaminants, which are mainly organic compounds and hydrocarbons, alter the refractive index or absorbance of the surrounding medium because they have absorption properties in the wavelength range of the sensor and can therefore influence measurements.

In oils with longer operating times, we noticed that the displacement of the RI and the average wavelength is shorter. This may indicate the presence of contaminants.

2.6 MODE RESONANCE IN OPTICAL STRUCTURES

In a general context, **mode resonance** occurs when certain physical and boundary conditions allow a specific electromagnetic field distribution—called a *mode*—to be amplified or propagated preferentially within a dielectric or metallic structure. This condition arises when the system satisfies **phase** and **amplitude** criteria that promote **constructive interference** of waves that propagate or reflect internally, resulting in efficient coupling of optical energy to one or more resonant modes of the structure (SALEH; TEICH, 2007; AGRAWAL, 2012).

A specific and particularly relevant type of this phenomenon is Loss Mode Resonance. Unlike other types of resonance—such as Surface Plasmon Resonance (SPR)—LMR occurs in dielectric or passive semiconductor materials, in which the imaginary part of the electrical permittivity (ε'') is not zero, but it also does not imply optical gain. This component represents the intrinsic losses of the material and is essential for the emergence of loss modes, which characterize the LMR. This phenomenon has aroused great interest in the field of optical sensing, as small variations in the dielectric properties of the coating—induced by changes in the refractive index, temperature, or chemical composition of the external medium—cause measurable shifts in the spectral position of the resonance. This spectral sensitivity makes LMR-based devices promising tools for the high-precision detection of gases, biomolecules, and physicochemical parameters (LIU, 2018).

2.6.1 Lossy Mode Resonance (LMR)

Lossy Mode Resonance is an optical resonance phenomenon widely exploited in the development of fiber optic-based sensors. This effect manifests itself when a dielectric substrate—typically an optical fiber with the cladding partially or totally removed—is coated with a thin film of a suitable material and comes into contact with another dielectric medium with a higher refractive index. The coating materials generally used to make thin films are metal oxides (such as indium tin oxide (ITO), titanium dioxide (TiO_2), and indium oxide (In_2O_3), or functional polymers, selected for their specific optical properties. The essential condition for LMR to occur is that the thin film material has a real part of positive dielectric permittivity and a magnitude significantly higher than the imaginary part and the permittivity of the surrounding medium. These thin film materials are characterized by having a real part of the permittivity that is positive and greater in magnitude than the imaginary part and the permittivity of the surrounding medium, resulting in "lossy modes" in the material. The real part of the permittivity being positive confirms that the material behaves essentially as a dielectric, allowing light to be "guided" within the thin film that coats it. If this real part is greater in magnitude than the imaginary part, it characterizes the fundamental condition for LMR-type materials. This means that, although there is some absorption or loss of energy in the material (given by the imaginary part), the dielectric effect (energy storage, given by the real part) is dominant. If the imaginary part were much larger, the material would be very conductive or absorbent, and light would not be able to form guided modes or would be rapidly attenuated. This specific relationship allows modes to couple from the evanescent wave of the fiber to the thin film, resulting in "attenuation dips" in the transmission spectrum, which are the signatures of LMR. (IMAS et al., 2023)

For coupling to occur and LMR to be generated, two main conditions are necessary:

mode field overlap and phase matching, which requires the real part of the propagation constants of the lossy modes and the waveguide modes to be equal.

2.6.2 Absorbance vs. Wavelength

Absorbance is the logarithmic measure of how much optical power is attenuated as light passes through a medium, defined as

$$A = -\log_{10}(T) = \log_{10}\left(\frac{I_0}{I}\right), \tag{6}$$

where T is the transmittance and I_0 and I represent the incident and transmitted optical intensities, respectively. In Loss Mode Resonance (LMR) systems, absorbance is intrinsic to the detection mechanism because resonance excitation in the thin film induces wavelength-dependent optical losses, which appear as resonance dips in the transmitted spectrum. This inherent reliance on absorbance introduces both performance limitations, such as reduced signal-to-noise ratio under high baseline attenuation, limited dynamic range due to resonance saturation, and sensitivity to optical source fluctuations, as well as calibration challenges, since accurate resonance tracking requires stable intensity referencing, baseline correction, and compensation for drift caused by temperature variations, optical alignment changes, and thin-film aging.

Absorbance, being intrinsic to detection in Loss Mode Resonance (LMR) systems, introduces both performance limitations and calibration challenges that are essential to the practical application of thin-film LMR sensors. Evanescent wave-based sensors, including LMRs, can exhibit relatively small detected signals, i.e., signals whose optical response of the sensor to changes in the external medium is of low amplitude due to limited interaction between the evanescent field and the analyte. Sensitivity per unit length is generally lower than that of a direct absorption cell, but can be partially compensated for by long interaction lengths in the optical fiber. At high concentrations of absorbing species, Beer-Lambert's Law may deviate from perfect linearity. This limits the useful operating range of the sensor and can make accurate measurements difficult, especially in scenarios with high absorbance, as observed in measurements with insulating oil. In experiments with aggressive liquids, the initial resonance depth may be small, making it difficult to determine the concentration with acceptable accuracy for certain ranges. If contaminants absorb light in the same wavelength range as the sensor resonance, this can affect the resonance depth. Although the imaginary part of the refractive index affects the resonance depth, the real part is primarily responsible for sensitivity and wavelength shift.

2.6.3 The Optical Sensor Based em Lossy Mode Resonance- LMR

When a thin film is deposited on a region of an optical fiber where the coating has been removed, the propagation of light is affected by the interaction of the fiber's evanescent field with the thin film. This interaction can generate different types of resonances, such as lossy mode resonance, depending on the refractive indices of the fiber, the film, and the surrounding medium. Materials such as metal oxides (e.g., ZnO, SnO_2,Tio_2) and polymers generally meet the conditions for generating LMRs (IMAS et al., 2023).

The position and depth of resonance are influenced by the real and imaginary parts of the film's refractive index, the thickness of the coating, and the refractive index of the surrounding medium (SRI). Common applications of LMR include stripped cladding multimode fibers (CRMF), adiabatic taper single-mode fibers (ATSMF), and D-shaped single-mode fibers, each with its own specific resonance characteristics. Surface plasmon resonance (SPR) is widely used in sensors/biosensors, but the combination of thin films of metal oxides or polymers with optical fibers has made it possible to exploit the LMR phenomenon for sensing, with notable applications in various fields (SPACCKOVA et al., 2018). Both mechanisms, SPR and LMR, use a thin layer of material to support their relative modes, with LMR relying on a thin film with a high refractive index deposited on a suitable substrate. The measurement of refractive index using optical devices based on lossy mode resonance, LMR type (see Figure 3), is common in the literature and is an effective method for chemical sensors and optical biosensors. The sensitivity of these devices depends on the optical characteristics of the coating material and the amplitude of the evanescent field (CHIAVAIOLI; JANNER, 2021).

Figura 3 – LMR Sensor

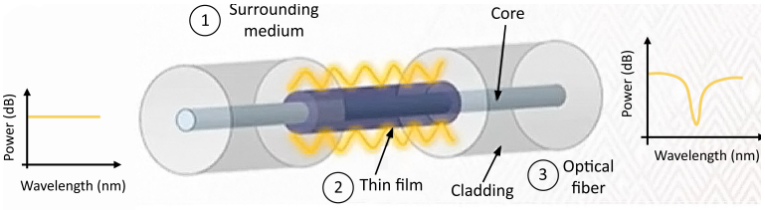

Source: Adapted from (IMAS et al., 2023)

2.7 GENERATION OF MULTIPLE RESONANCES

Optical sensors based on lossy mode resonance (LMR) can exhibit multiple resonances in the transmission or reflection spectrum when modal confinement conditions allow simultaneous coupling between different guided optical modes and lossy modes existing in the thin film deposited on the substrate. The generation of these multiple resonances is strongly associated with the coating thickness, spectral dispersion, and dielectric properties of

the material used, which determine the number of modes supported and the spectral position of each resonance (VILLAR et al., 2017). Thus, controlled variations in film thickness or optical permittivity of the material can induce the appearance of several resonance peaks, each corresponding to a distinct coupling between the propagating mode of the fiber and the loss modes of the coating. These multiple peaks offer greater flexibility for simultaneous monitoring of different parameters or for improving the spectral sensitivity of the sensor. From a physical point of view, this behavior can be interpreted based on modal coupling theory and the propagation of evanescent waves in stratified media, in which the interaction between the evanescent field and the cladding produces different resonant phase conditions. Recent studies show that optimizing these multiple LMRs allows for an increase in dynamic range and a reduction in the influence of instrumental noise, consolidating this technique as a promising alternative to traditional plasmonic sensors (AGRAWAL, 2012).

The ability to generate multiple LMR resonances in the same fiber without altering its geometry allows the creation of sensors with multiple reference points or for filtering multiple wavelengths (PALIWAL; JOHN, 2015).

Figura 4 – Representation of Multiple Resonances

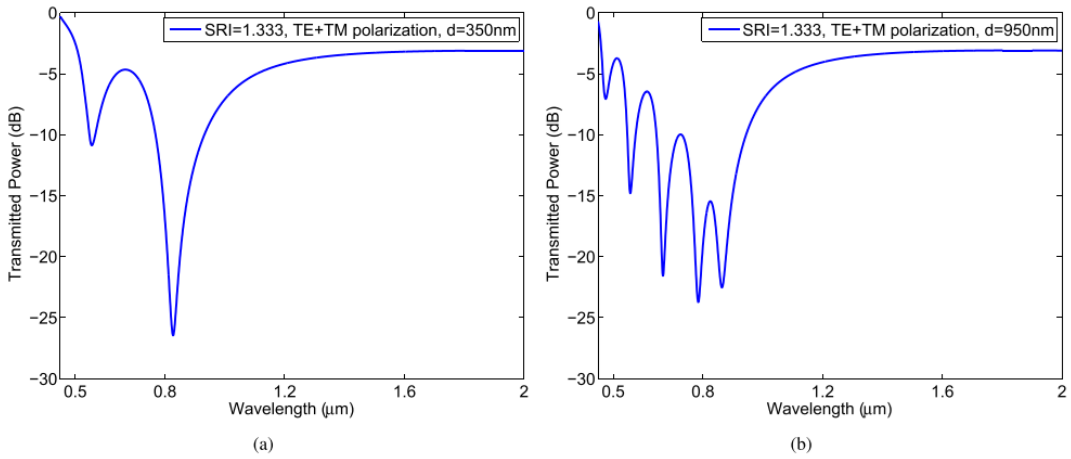

Source: Adapted from (PALIWAL; JOHN, 2015)

Such sensors can be developed with different coating materials, the choice of which directly determines their detection characteristics and specific areas of application. Among the main examples reported in the literature, the following stand out:

- Aluminum-Doped Zinc Oxide (AZO): Combined with TiO_2 (AZO/TiO_2), it can offer improved sensitivity compared to single layers.
- Silver Nanoparticles: Films loaded with them are exploited for monitoring human respiration.

- Molybdenum disulfide (MoS_2)/Graphene: Used in the detection of NO_2.
- ZnTe/Bi_2Te_3: A heterostructure that has also been explored for LMR sensors.

3 RELATED WORKS

This chapter aims to present the state of the art in the field of optical sensing, with special emphasis on the applications of Loss Mode Resonance technology, highlighting the relevance and potential of these technologies for the development of future applications. It also presents the state of the art in the use of advanced materials and composites in the design of multiparametric systems, highlighting the possibilities for application in various areas of engineering and science.

3.1 FIBER OPTIC SENSORS FOR FLUID MONITORING

Monitoring the operational conditions of insulating oil in power transformers is an essential practice for assessing reliability and extending equipment service life (LU et al., 2019). Among the emerging technologies applied in this context, fiber-optic sensors stand out as promising alternatives due to their electromagnetic immunity, compact dimensions, chemical resistance, and ability to operate in harsh environments. These devices have been extensively researched and developed for measuring critical parameters such as temperature, partial discharges, and dissolved gas concentrations, including specific compounds such as furfuraldehyde. Measuring the internal temperature of transformers is a fundamental parameter for diagnosing their service life, since thermal aging is directly associated with the degradation of the oil-impregnated insulating paper. Conventional measurement techniques, which rely on indirect assessment, often present significant discrepancies. In this context, fiber-optic sensors offer a robust solution, enabling direct temperature measurements in the transformer windings, either at discrete points or in distributed configurations (IEC 60599, 2015).

A study highlighting the use of Fiber Bragg Grating (FBG) sensors in oil and gas wells for monitoring multiple parameters was conducted in 2012 (AL-FAKIH et al., 2012). The use of FBGs is fundamental for temperature measurement in subsea oil exploration applications and is classified for the energy industry (oil and gas) to measure temperature, pressure, and flow. FBGs are used to measure physical effects such as temperature, pressure, chemical composition, deformation, and acoustics in oil and gas wells. For well applications, FBG sensors are designed to withstand harsh environments, with temperature measurement in fluids being a key parameter. FBGS were also used in a hot spot detection system for oil and gas pipelines in the study proposed by Wang (WANG et al., 2020). A practical and reliable distributed hot spot detection system was proposed and demonstrated using an array of ultrasensitive FBGs in combination with the OTDR (Optical Time-Domain Reflectometry) technique. This system is considered significant for pipeline monitoring applications. The method has a temperature

measurement accuracy of ±1 °C and is suitable for early warning of centimeter-sized fire sources in some pipeline monitoring applications.

The phenomenon of partial discharges is one of the main causes of incipient faults in transformers (MEITEI; BORAH, 2023). To detect them, new techniques are being investigated using fiber optic ultrasonic sensors. These systems usually consist of an optoelectronic acoustic probe connected to a digital signal processor. Optical fiber is used as a transmission medium between the probe and the processor, providing greater immunity to external noise. Analysis of gases dissolved in insulating oil (DGA) it is one of the most widely used techniques for diagnosing internal faults in transformers. In this field, there is growing interest in the application of fiber optic-based optoelectronic sensors, mainly due to their high electromagnetic immunity and feasibility for direct insertion into the equipment.

Long-period network-based fiber optic sensors (LPGS) and interferometric structures have been explored mainly for the evaluation of liquid fuels, such as ethanol, gasoline, and biodiesel. However, their characteristics—such as small size, electrical and chemical passivity, electromagnetic immunity, low response time, and resistance to hostile environments—also make them suitable for monitoring insulating oil, a petroleum derivative. LPGs are particularly sensitive to variations in the refractive index of the external medium, a property that allows them to identify changes in the composition and degradation of liquids. Structures such as the Mach-Zehnder interferometer (two LPGs in series) and the Michelson interferometer, also known as self-interfering LPG (SILPG), enhance the sensitivity of detection (POSSETTI, 2013).

The operating principle of LMR-based sensors, as well as their performance, is directly related to the appropriate selection of materials used in thin film deposition. Materials such as certain oxides, for example, can significantly optimize sensor sensitivity and efficiency, enabling considerable improvement in monitoring and detection applications (PALIWAL; JOHN, 2015).

A wide range of fiber coating materials has been shown to be suitable for the implementation of LMRs, provided that the real part of the dielectric constant of the film material is positive, exceeds its imaginary part in absolute value, and is greater than the same parameter of the dielectric waveguide and the environment. Materials such as ITO , In_2O_3, TiO_2, Al_2O_3, SnO_2, and some polymers meet these criteria. Such materials are chemically resistant, making them ideal for sensors in aggressive gases and liquids.

Indium Tin Oxide films have the ability to generate multiple resonances without the need for any modification to the fiber geometry. In addition, their sensitivity can be significantly influenced by the thickness of the thin ITO film, allowing for precise adjustments for different applications. They are particularly suitable for generating LMR in the VIS-NIR spectral range (400–1366 nm), which expands the possibilities for using these devices (ZUBIATE et al., 2016).

Lossy mode resonances sensors have great potential for monitoring in chemically aggressive environments, such as concentrated acid and alkali solutions (KUZNETSOV et al., 2021). A sensor based on a single-mode optical fiber with a chemically etched coating, covered with a thin film of tin dioxide (SnO_2) by metalorganic vapor deposition showed satisfactory results when used in aggressive environments such as aqueous HCl (hydrochloric acid) solutions, HNO_3 (Nitric Acid), H_2SO_4(Sulfuric Acid) and NaOH (Sodium hydroxide, commonly known as caustic soda). The high chemical durability of the coating was confirmed by its insensitivity to aqua regia, which is a highly corrosive mixture formed by combining two strong acids (HCl + HNO3).

Kuznetsov's study (KUZNETSOV et al., 2021) presented the unprecedented determination of the molar concentration and refractive index of strong acids and bases HCl, HNO_3, H_2SO_4, NaOH using the position of the first LMR. This propagation mode is generally more sensitive to variations in the external refractive index. These applications confirm the effectiveness of the sensor as a fiber optic refractometer, exhibiting linear dependence in the short operating range, demonstrating that it provides a chemically durable and highly sensitive solution. It also allowed the monitoring of aggressive liquids, introducing the unprecedented ability to simultaneously quantify molar concentration and refractive index.

Since transformers operate under severe thermal, electrical, and mechanical stresses, this condition makes them susceptible to failures such as mechanical deformation of windings and cores, partial discharge, overheating, and electric arcing. Early detection is vital to avoid catastrophic consequences. Monitoring the condition of power transformers is an increasingly important topic in electrical engineering, especially given the need to ensure the reliability of power transmission and distribution systems. A survey conducted in Australia between 2000 and 2015 revealed that 3,29% of the transformers evaluated had failures, with windings accounting for approximately 50% of cases, followed by on-load tap changers, which accounted for 15% of occurrences (JIN et al., 2022).

Given this need, several sensor studies have emerged with the aim of monitoring the conditions of insulating oil in transformers. In the study presented by Filho, portable microcontrolled equipment is developed for online detection of gases dissolved in transformer oil (FILHO et al.,). The proposed equipment consists of an electronic system with decision-making capabilities and coupled to an infrared emission and reception system, in order to monitor and identify the main gases dissolved in transformer oils (carbon dioxide, methane, ethylene, and propane). This device can be connected to the oil drain outlet of power transformers and automatically identifies the aforementioned gases dissolved in the oil as soon as they appear. This equipment is currently under development and has not yet been commercially distributed.

Several technologies have been proposed to meet these demands; however, optical

sensors stand out for their robustness, resistance to harsh environments, and high sensitivity. Among them, devices based on lossy mode resonance (LMR) have received increasing attention in recent years, as they offer superior performance compared to conventional optical sensors (VITORIA et al., 2023).

The use of the LMR sensor in investigating the conditions of insulating oil has been widely studied. In this regard, the work presented in this dissertation applies the LMR sensor to the offline analysis of insulating oils under real operating conditions in the electrical system and seeks to correlate the refractive index with other conditions previously identified in the physical-chemical analyses of these fluids.

4 CHARACTERIZATION AND CALIBRATION OF THE LMR SENSOR

Chapter 4 will discuss the methodologies used to characterize the LMR sensor and enable its use as a refractometer to analyze the conditions of mineral oil in transformers, taking into account mainly the aging of insulating oil. To this end, an experimental bench arrangement was developed that enabled the calibration of the sensor and the survey of its calibration curve, using solutions with different concentrations of glycerin and water. Measurements were taken at room temperature of these different concentrations. Deionized water was used, for which the refractive index was already known (n= 1.33), and five measurements were taken on five samples, a quantity chosen because it is commonly adopted in experimental studies and has been used in previously published works in the literature. Varying the water/glycerin concentration in the following proportions: H2O 100%, 30% glycerin, 50% glycerin, 70% glycerin, and 100% glycerin. These values were chosen because it would be necessary to characterize the sensor within a calibration range covering the refractive index up to 1.48 RI, which is the range of refractive index values of insulating mineral oils commonly used in power transformer insulation. Five measurements were taken in each solution. After each measurement, the sensor was cleaned and its spectrum was measured with white light and compared with the value and curve obtained in its initial state (clean and dry sensor). This process was repeated for each measurement. For the measurements of the refractive index of the insulating mineral oil, four samples were used, named samples “A, B, C, and D.” These oil samples were collected from equipment in different operating conditions and with different degrees of aging. Five measurements were taken for each of the four samples. The procedure of sanitizing the sensor after each measurement and checking the detection condition by comparing its spectral curve with the curve obtained in its initial stage (dry sensor and in the air) was strictly repeated at each stage of the test.

4.1 MATERIALS AND EQUIPMENT

Section 4.1 presents a description of the materials and equipment used, as well as the configurations made for the experiments. All equipment used belongs to the Multi-user Photonics Laboratory - FOTON located at the Federal Technological University of Paraná (UTFPR).

4.1.1 Ocean Optics QE65000O Spectrometer

The operating principle of the QE65000 is based on the dispersion of light or electromagnetic radiation at different wavelengths and the detection and analysis of these wavelengths. Light or electromagnetic radiation is emitted from a source, which can be a lamp, laser, or synchrotron radiation. This light is directed through a collimator that transforms it into a parallel beam. The beam then passes through a dispersive element, such as a prism or diffraction grating, which separates the light into its components of different wavelengths. These wavelengths are then directed to a detector that converts the scattered light into electrical signals, which are then amplified and digitized. The digitized signal is processed by a computer, which generates a spectrum. This spectrum is represented by a graph showing the intensity of light as a function of wavelength (PAVIA et al., 2010).

The Ocean Optics QE65000 Spectrometer has a wavelength calibration error of approximately ±0.1 nm and an accuracy of ±0.05 nm. It is known for its high quantum efficiency, reaching up to 90%. The Hamamatsu detector has excellent response in the ultraviolet range, with a spectral response range of **200 nm to 1100 nm**.

Figura 5 – Quantum Efficiency of the QE65000 Detector

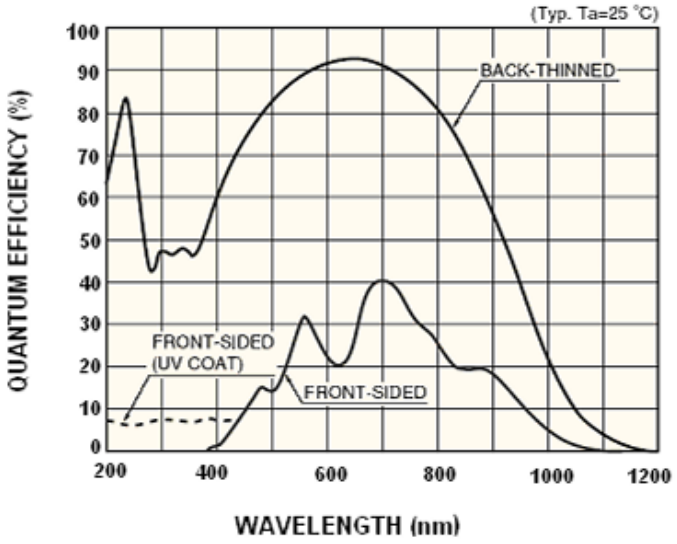

Source: Adapted from (MANUAL, 2015)

The Ocean Optics QE65000 used in this experiment is a highly sensitive spectrometer designed for applications requiring low light levels, such as fluorescence, DNA sequencing, astronomy, and Raman spectroscopy. Features:

- Quantum Efficiency: Up to 90%;
- Detector: Hamamatsu back-thinned with excellent response in the ultraviolet range;

- Pixel arrangement: 2-D (1044 horizontal x 64 vertical);
- Response Range: 200 nm to 1100 nm;
- Noise Reduction: The detector has grouped columns to minimize reading noise;
- Cooling: Can be cooled to -10°C to reduce thermal noise;
- A/D converter: 16 bits, with a signal-to-noise ratio of >1000:1;
- Interface: USB 2.0 and RS-232;
- Integration Time: Up to 10 minutes, which improves the detection limit in low-light applications.

The QE65000 is ideal for applications requiring high sensitivity and low noise, providing accurate and reliable results.

4.1.2 AQ4305 White Light Source

The Light Source AQ4305 is a device used to measure the wavelength loss characteristics of optical devices and optical fibers. Operating Steps:

1. White Light Source: The AQ4305 emits incoherent white light, which is a combination of different wavelengths of visible and near-infrared light.
2. Wavelength Loss Measurement: White light is passed through the device or optical fiber being tested. The equipment measures how light is absorbed or lost along the way, which helps to understand the properties of the device or fiber.
3. Stability and Accuracy: The AQ4305 provides highly stable optical outputs with minimal variation, ensuring accurate and reliable measurements.
4. Use in Conjunction with Optical Spectrum Analyzer: For best results, the AQ4305 is often used in conjunction with an optical spectrum analyzer, which helps analyze scattered light and provide detailed data on wavelength loss. In this experiment, the spectrometer mentioned in section 4.1.1 was used. The results obtained were as follows: In this experiment, the spectrometer mentioned in section 4.1.1 was used.

The Yokogawa AQ4305 White Light Source has an accuracy of ±0.05 dB and an optical output stability error of ±0.05 dB. It is designed to measure wavelength-dependent loss characteristics of optical devices and optical fibers in conjunction with an optical spectrum analyzer.

Figura 6 – The typical optical output of the AQ4305

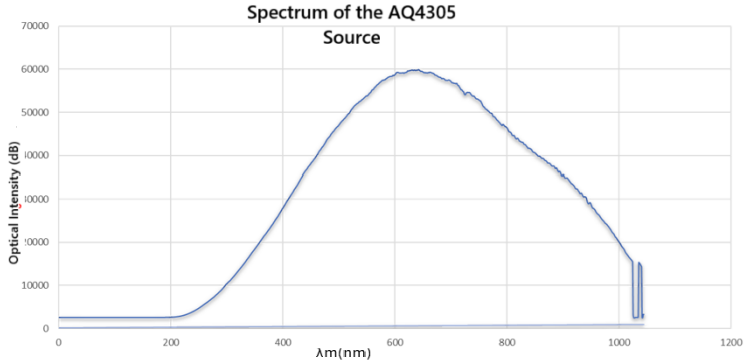

Source: Software - Spectra Suite

4.1.3 SpectraSuite Software

SpectraSuite is modular, Java-based software developed by Ocean Optics to control USB spectrometers and other USB instrumentation devices. It runs on Windows, Macintosh, and Linux operating systems. Key Features:

- Modularity: The software consists of modules that can be added or removed as needed, allowing you to customize the interface and functionality.
- Device Control: You can control multiple Ocean Optics USB spectrometers and devices from other manufacturers, provided the appropriate drivers are installed.
- Advanced Measurements: Supports absorption, emission, transmission, and reflection measurements, as well as techniques such as dual-beam reference and process monitoring
- Customizable Interface: All visual and functional aspects of the interface can be modified, allowing the creation of a fully customized application.
- Data Capture: Enables advanced episodic data capture, storing data at a speed of up to one scan per millisecond.

This software was fundamental in the process of acquiring data from the experiment in question. First, the software was installed on the computer, then the spectrometer was connected via USB. The next step was to configure the software to control the device, adjusting parameters such as wavelength, integration time, and measurement type. Once this was done, the data collection was displayed on the screen, graphically and numerically in the software. The analysis of the collected data was performed in conjunction with a Python code developed specifically for this purpose. Through this analysis, it was possible to obtain information about the properties of the material and the solutions tested.

Figura 7 – LMR Sensor Characterized in SpectraSuite

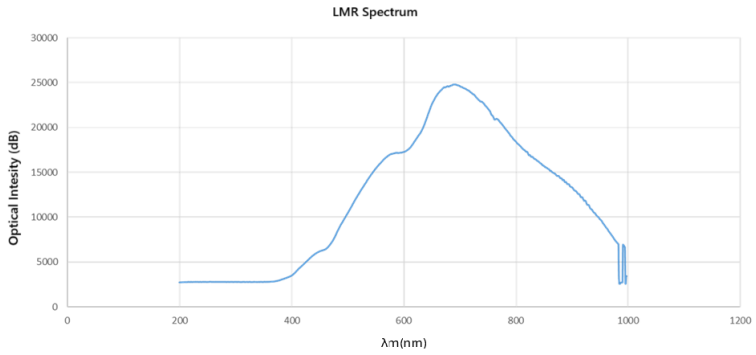

Source: Own authorship

4.1.4 Python Code

A Python code was developed, in collaboration with an undergraduate student, to process and analyze the data collected by the SpectraSuite software. The main functions of the software are listed in its interface menu, as shown in Figure 8:

Figura 8 – Python Code Menu

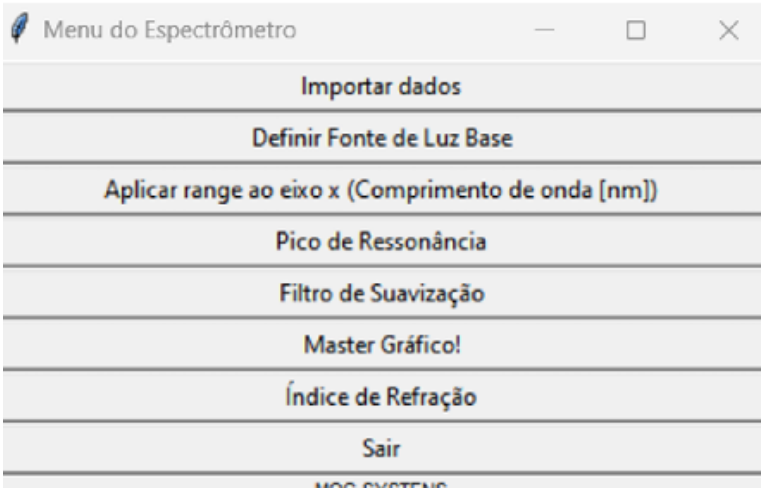

Source: (ASSIS; CAMARGO, 2024)

- Import data: this function allows you to import data from .xls files, obtained by SpectraSuite, and add them to your database. The user selects the files to import. The data is then saved in a specific folder, which will always be accessed when necessary. This function is the first step in preparing the data for further analysis by the script.
- Define Base Light Source: the “Define Base Light Source” function is important for obtaining a reference point in subsequent analyses. It allows the user to choose an .xlsx file that must contain the spectrum data of the light source used, in this case the AQ4305 source, without the LMR sensor. This data is used to differentiate between

the base spectrum and the data from the fiber optic spectra with the sensor. This way, the functions that show the LMR resonance spectrum display only peaks of the LMR resonance wavelengths, instead of absorption valleys in the light source spectrum. This facilitates visualization and analysis.

- X-Axis Interval Configuration (Wavelength [nm]): This feature allows the user to define a custom interval for the x-axis, representing the wavelength in nanometers, as needed. This customization is useful for focusing on a specific range of wavelengths for analysis.
- Resonance Peak Selection: This function is used to select which LMR resonance peak will be analyzed, assisting in the smoothing filter process. The user can decide between the second or third resonance peak. Initially, the script is configured to focus on the second peak.
- Smoothing Filter: This function applies the Savitzky-Golay filter to smooth the data and reduce noise, focusing on resonance peaks defined by the user. The Savitzky-Golay filter uses a local fitting polynomial to smooth the data, automatically adjusting the filter window size and the polynomial order to ensure the best possible smoothing.This filter is essential for accurate analysis of resonance peaks. When activated, this function applies the filtering process to all displayed graphs, as shown in Figure 9.

Figura 9 – Python Smoothing Filter

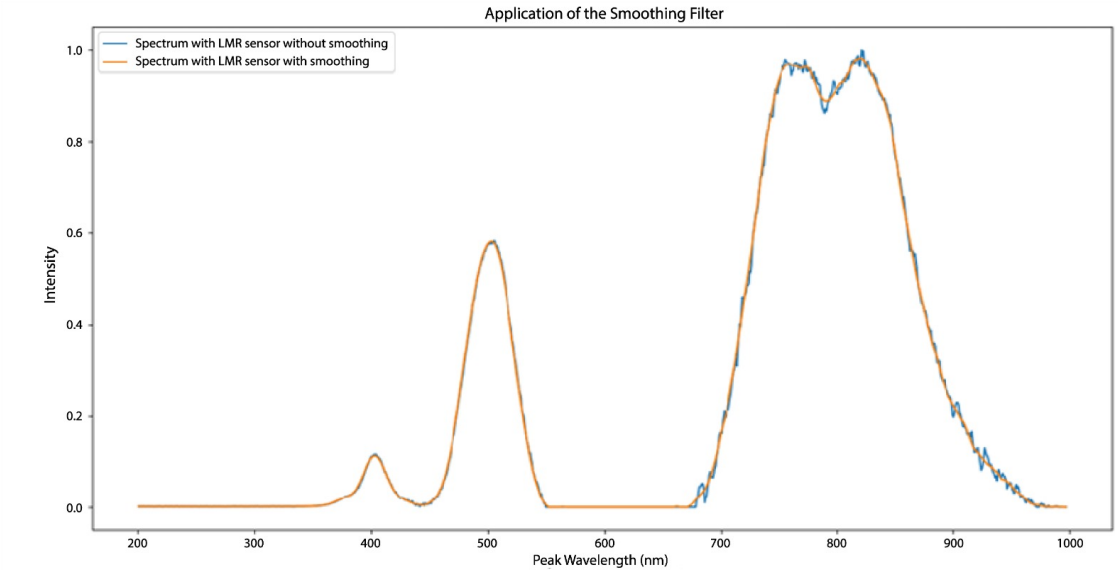

Source: Own authorship

- Master Graph: This function compiles all stored spectra and performs the subtraction of the baseline spectrum, generating a consolidated graph. Its execution depends on the smoothing filter routines, resonance peak detection, and x-axis interval definition, which directly influence the shape of the resulting graph. After generating the master

graph, the results are saved in a single .xlsx file, which facilitates the analysis of LMR resonance spectra. In the figure below, the tests performed with the LMR sensor under different conditions are presented: sensor in air, sensor immersed in water, and in different concentrations of the water–glycerin mixture. It can be observed that each spectrum is well characterized, showing a spectral shift from the orange region to the red region, with peaks concentrated at wavelengths between 600 and 700 nm (see Figure 10 – Master Graph).

Figura 10 – Python Master Chart

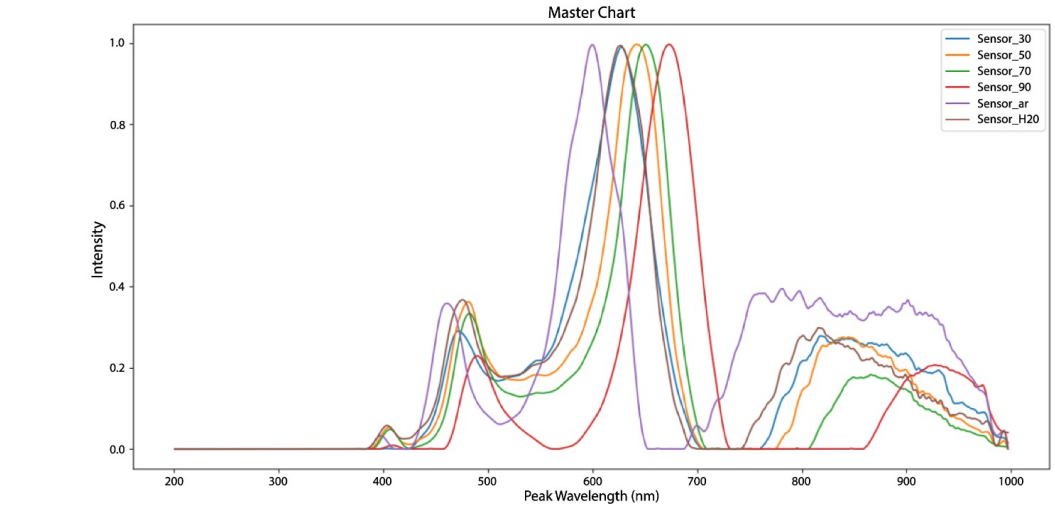

Source: Own authorship

- Refractive Index: This function uses the master graph to identify the wavelengths at the LMR resonance intensity peaks, as defined by the resonance peak function. The peak values are then saved in an .xlsx file and plotted on a graph correlating the refractive indices with the LMR resonance peaks, which is essential for accurate analysis of the spectral data.
- Data Normalization: An integral part of the script, this function adjusts the measured values to a common scale (0 to 1), improving the visualization of intensities. It operates automatically within the script, converting all data, calculating minimum and maximum values of the spectra, and applying normalization. Normalization is essential to avoid parameterization errors and ensure the correct functioning of the script.

4.1.5 Experimental Setup

The experimental setup consisted of the AQ4305 white light source. This source, through its halogen lamp, emits a beam of light that passes through the optical fiber to the

LMR sensor. This sensor was manufactured in a multimode fiber, with an exposed core and a zinc oxide deposition, using the sputtering technique. The sensor was manufactured in Spain, in a collaborative project between the Federal Technological University of Paraná and the Public University of Navarra (see Appendix B). The sensor remains immersed in the H_2O and glycerin solution. This arrangement allows for variation in the refractive index through the use of different H_2O /glycerin solutions. The light that interacts with the sensor is then conducted through the optical fiber to the QE6500 spectrometer. The spectrometer analyzes the transmitted spectrum with the support of SpectraSuite software. At this stage, the data is collected and sent to a computer via USB, on which the "Python Code" is installed, which processes the data and enables its graphical analysis. The experimental setup allowed for the proper calibration of the sensor and the mapping of its calibration curves. Using solutions with different concentrations of glycerin and water, measurements were performed at room temperature. The experimental setup allowed for proper calibration of the sensor and the mapping of its calibration curves. Using solutions with different concentrations of glycerin and water, measurements were taken at room temperature. Deionized water was used, whose refractive index is known (n=1.33). Five measurements were taken on five samples, varying the water/glycerin concentration in the following proportions: 100% H2O, 30% glycerin, 50% glycerin, 70% glycerin, and 100% glycerin. These values and proportions for the tested solutions were chosen because they are commonly used in optical fiber sensor calibration experiments, as evidenced in other publications.Also these proportions allowed the sensors to be characterized in a calibration range covering up to 1.48 RI, equivalent to the refractive index of mineral insulating oils commonly used in power transformers. Five measurements were taken in each solution. After each measurement, the sensor was cleaned and its spectrum measured with white light was compared with the value obtained in its initial state (clean and dry sensor).

Figura 11 – Experimental Setup

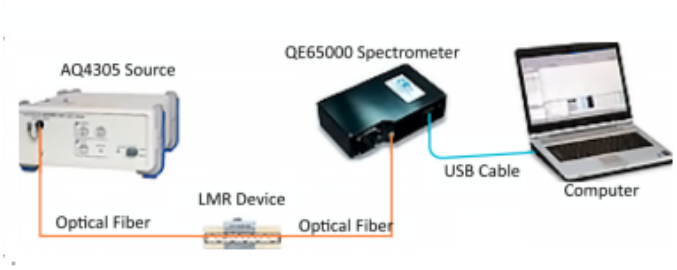

Source: Own Authorship

4.2 LMR SENSOR CALIBRATION CURVE

The characterized and calibrated sensor was a device made of multimode optical fiber with a core diameter of 150 µm (Thorlabs FT200UMT), core diameter, with the cladding removed, measuring 2 cm x 1 cm x 3 mm in length, width, and thickness, covered with a thin film of ZnO (zinc oxide). According to the coupling mode theory, loss mode resonance (LMR) is generated due to the coupling of light between the evanescent wave and the guided modes with losses in the thin film. This coupling depends mainly on the thickness of the thin film layer. The LMR sensors were manufactured using the metal oxide thin film deposition method known as sputtering, explained in detail in specific literature (ZUBIATE et al., 2016).

To calibrate the sensor using Python code and the peak detection method, it was observed that the best curve was obtained with untreated data for this sensor. * In this case, the code already considers the refractometer error = 0.0002.

Figura 12 – LMR Sensor Calibration

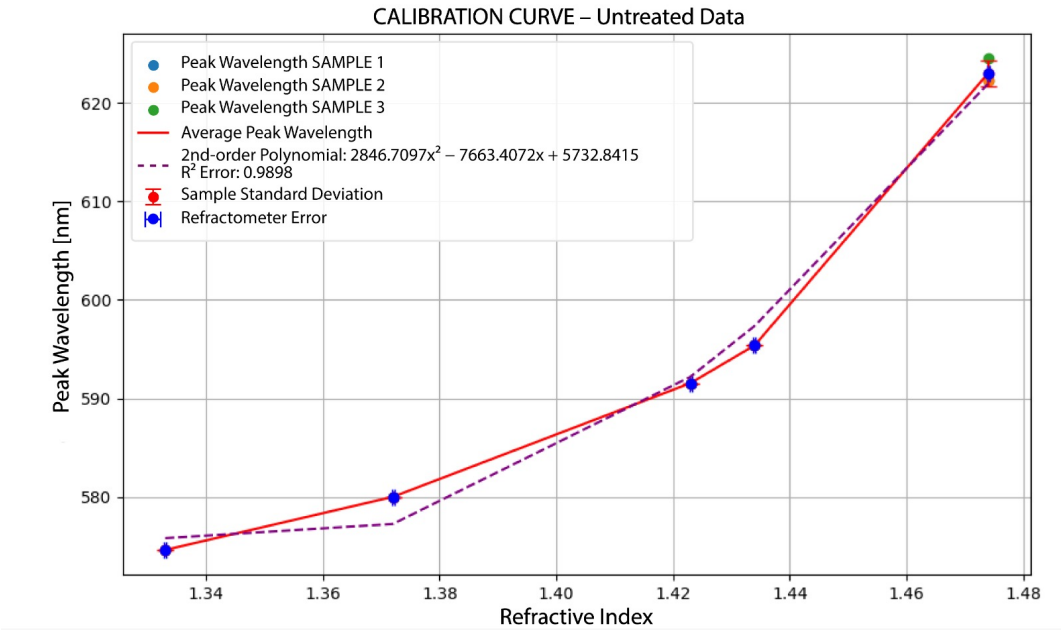

Source: Own Authorship

The graph shown in Figure 12 represents the calibration curve of the LMR Sensor studied. The equation shown represents the polynomial function that calculates the refractive index (x-axis) as a function of the measured wavelength (y-axis). The wavelength used is λm which represents the average wavelength of the three measurements taken at each of the sensors, IR is the refractive index solution. The average error is calculated by dividing the standard deviation by the square root of the sample size, in this case five (5) samples, which would be the water and glycerin solutions at different concentrations.

Figura 13 – Transmitted Spectrum LMR Sensor Calibration - Python

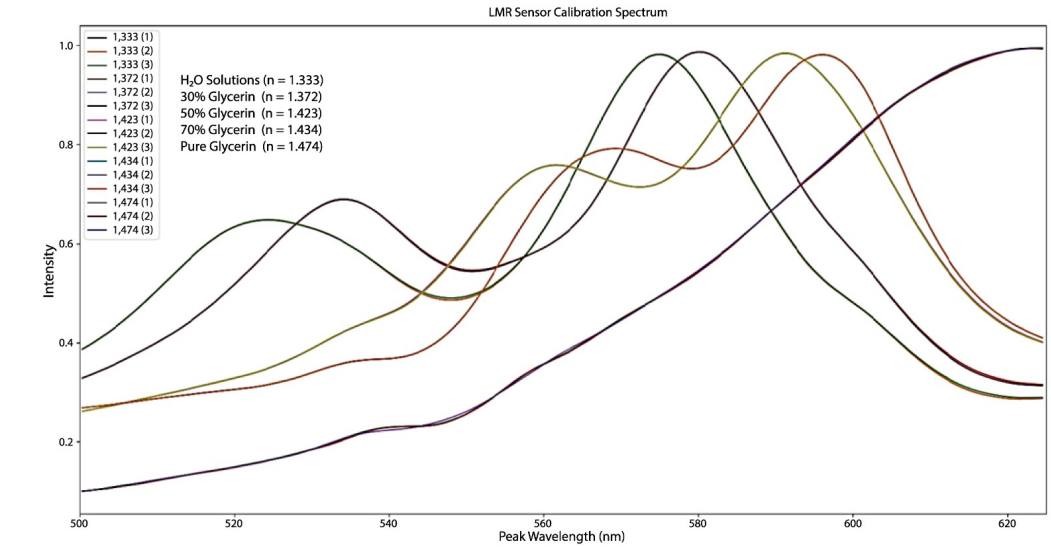

Source: Own Authorship

Figure 13 shows the transmitted spectrum of the sensor at different solution concentrations. The refractive index values of water and other water-glycerin concentrations were previously measured in the laboratory using a device called a refractometer. These values were considered as reference values for the experiments. In this image, the spectra were filtered in Python code for a range of 500 nm to 620 nm. In this figure, it is possible to observe the shift of the peaks to the right. It is also possible to observe that the wavelength (λ) varied from 574.61 nm to 623.02 nm, in this case within the characteristic range of this device (ZnO). Figure 14 presents the LMR sensor calibration report generated by the Python code. The report shows the wavelength shift for each tested solution. In addition, the code provides the polynomial equation that characterizes the calibration curve.

Figura 14 – LMR Sensor Calibration Report - Python

RI	1.333	1.372	1.423	1.434	1.474
Peak wavelength [nm] - Untreated	574,61	580,00	591,55	595,39	622,26
Peak wavelength [nm] - Untreated	574,61	580,00	591,55	595,39	622,26
Peak wavelength [nm] - Untreated	574,61	580,00	591,55	595,39	624,55
Peak wavelength [nm] - Untreated - Medium	574,61	580,00	591,55	595,39	623,02
SAMPLE STANDARD DEVIATION	0	0	0	0	1,322132

```
Second-order polynomial: 2846.7097x²-7663.4072x+5732.8415
R² error: 0.9898
Refractometer error: ±0.0002
Using the peak detection method: No treatment
```

Source: Own Authorship

With regard to device sensitivity, it can be said that the higher the sensitivity value (nm/RIU), the greater the shift in the resonance wavelength for a given change in the measured property, which generally facilitates the detection of this change. As discussed in (PALIWAL;

JOHN, 2015), the sensitivity of an LMR sensor is mainly influenced by three factors:

- The refractive index of the thin layer.
- The thickness of the thin layer.
- The refractive index of the surrounding medium.

Increasing the refractive index of the thin layer and its thickness, as well as the refractive index of the surrounding medium, generally increases sensitivity, especially for the first resonance obtained. The thickness of the thin layer can also be used to adjust the position of the resonance at the desired wavelength. For the sensor studied, we obtained the following sensitivity value:

LMR Sensor

$$\text{Sensitivity} = \frac{623{,}02\,\text{nm} - 574{,}61\,\text{nm}}{1{,}474 - 1{,}333} = \frac{48{,}41\,\text{nm}}{0{,}14} = 345{,}78\,\text{nm/RIU} \tag{7}$$

which in practice means that for each variation of 1 refractive index unit (1 RIU), the sensor's resonance peak shifts 345.78 nanometers in the spectrum.

5 CALIBRATION OF THE LMR SENSOR WITH TEMPERATURE VARIATION AND TESTS WITH INSULATING OIL

In this chapter, we will present the calibration tests of the sensor characterized in Chapter 5, subjected to thermal cycles ranging from 25°C, 45°C to 65°C, in water and glycerin solutions (H2O, 30% glycerin, 50% glycerin, 70% glycerin, and pure glycerin). We will also present the results of tests performed with temperature variation in insulating oil samples at a temperature of 60 °C, as this is a temperature close to the nominal operating temperature measured in the core of transformers, simulating real operating conditions.

5.1 INITIAL CONSIDERATIONS

In this chapter, we will present tests performed on samples of insulating oil from transformers in operation, under different operating conditions and states of degradation, using Sensor 3. This device was made of multimode optical fiber with 150 μm (Thorlabs FT200UMT), core diameter, with the peel removed, measuring 2 cm x 1 cm x 3 mm in length, width, and thickness, covered with a thin film of ZnO, previously calibrated, called Sensor 3, coated with zinc oxide and a fiber core diameter of 150 μmThe experimental setup included an AQ4305 white light source (Yokogawa) and an Ocean Optics QE65000 spectrometer. Calibration and temperature variation tests are shown in Figure 15 (a and b).

Figura 15 – Experimental Setup with Calibration (a) and Temperature Variation (b)

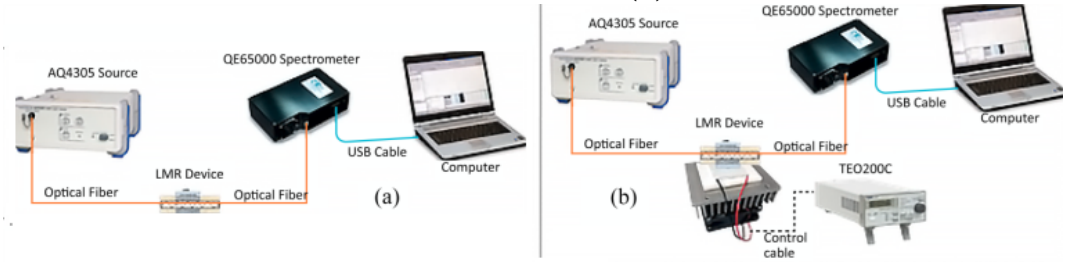

Source: Own Authorship

In this stage, the LMR sensor was calibrated at different temperatures. Calibration curves were plotted at temperatures of25°C, 45 °C and 65 °C, in water and glycerin solutions (H_2O, 30% glycerin, 50% glycerin, 70% glycerin, and pure glycerin).

The purpose of these tests was to show that the LMR device can be used in environments with temperature variations and maintain its refractometer characteristics. Figure 16 shows the calibration graph of the LMR sensor at a temperature of 25°C.

LMR Sensor 25 °C

Figura 16 – LMR Sensor Calibration Curve at Temperature 25°C

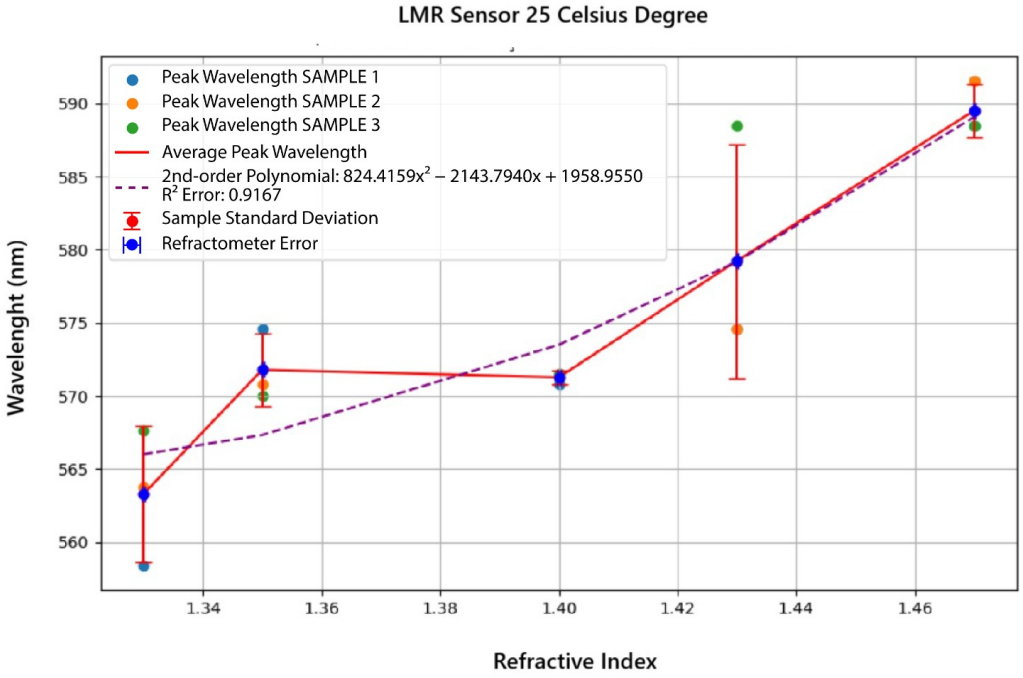

Source: Own authorship

Figura 17 – LMR Calibration Report at Temperature 25°C

RI	1.33	1.35	1.40	1.43	1.47
PICO wavelength [nm] - No treatment	558,41	574,61	570,76	574,61	588,47
PICO wavelength [nm] - No treatment	563,81	570,76	571,53	574,61	591,55
PICO wavelength [nm] - No treatment	567,67	569,99	571,53	588,47	588,47
PICO wavelength [nm] - No treatment - AVERAGE	563,30	571,79	571,27	579,23	589,50
SAMPLE STANDARD DEVIATION	4,65	2,48	0,44	8,00	1,78

```
Second-order polynomial: 824.4159x²-2143.7940x+1958.9550
R² error: 0.9167
Refractometer error: ±0.0002
Using the peak detection method: No treatments
```

Source: Own authorship

$$\text{Sensitivity} = \frac{589{,}49\,\text{nm} - 563{,}29\,\text{nm}}{1{,}474 - 1{,}333} = \frac{26{,}20\,\text{nm}}{0{,}14} = 187{,}07\,\text{nm/RIU} \tag{8}$$

which in practice means that for each variation of 1 refractive index unit (1 RIU), the sensor's resonance peak shifts 187.07 nanometers in the spectrum.

At this stage, the sensor was tested at 45°C (see Figure 18).

LMR Sensor 45 °C

Figura 18 – LMR Sensor Calibration Curve at Temperature 45°C

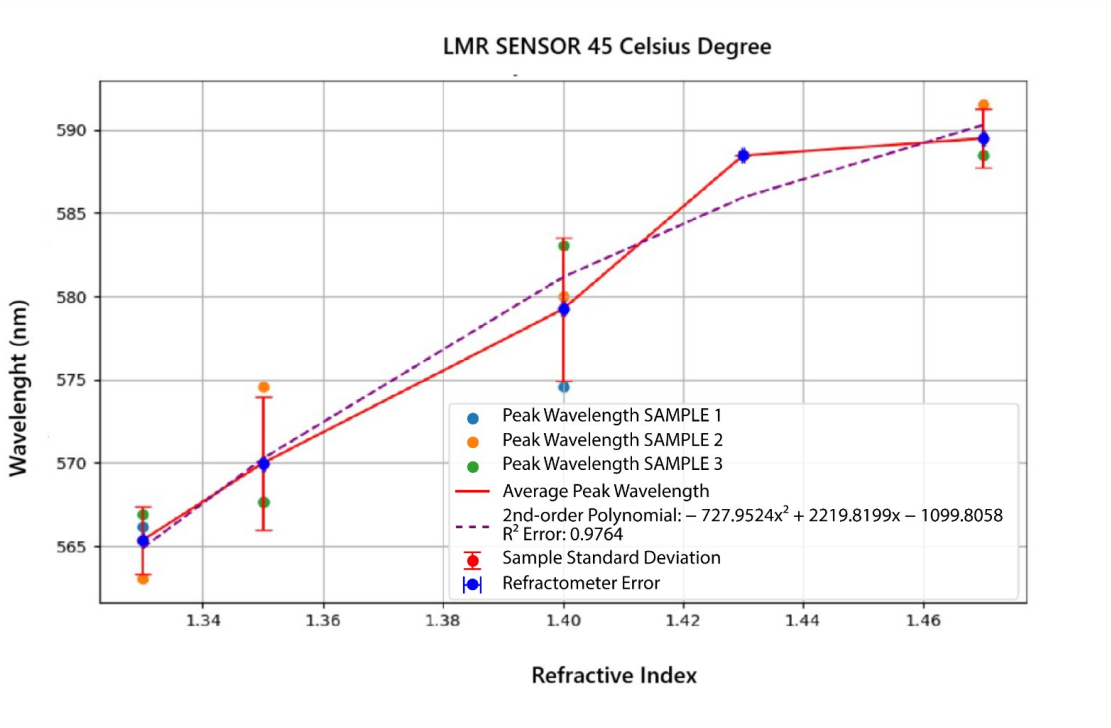

Source: Own authorship

Figura 19 – LMR Calibration Report at Temperature 45°C

RI	1.33	1.35	1.40	1.43	1.47
PICO wavelength [nm] - No treatment	566,13	567,67	574,61	588,47	588,47
PICO wavelength [nm] - No treatment	563,04	574,61	580,00	588,47	591,55
PICO wavelength [nm] - No treatment	566,90	567,67	583,08	588,47	588,47
PICO wavelength [nm] - No treatment - AVERAGE	565,36	569,98	579,23	588,47	589,50
SAMPLE STANDARD DEVIATION	2,04	4,01	4,29	0,00	1,78

```
Second-order polynomial: -727.9524x²+2219.8199x-1099.8058
R² error: 0.9764
Refractometer error: ±0.0002
Using the peak detection method: No treatment
```

Source: Own authorship

$$\text{Sensitivity} = \frac{589{,}50\,\text{nm} - 565{,}36\,\text{nm}}{1{,}474 - 1{,}333} = \frac{24{,}14\,\text{nm}}{0{,}14} = 172{,}42\,\text{nm/RIU} \tag{9}$$

which in practice means that for each variation of 1 refractive index unit (1 RIU), the sensor's resonance peak shifts 172.42 nanometers in the spectrum. Figure 19 shows the calibration report generated by Python code.

Figure 20 shows the calibration graph for the LMR sensor at a temperature of 65°C.

Figura 20 – LMR Sensor Calibration Curve at Temperature 65°C

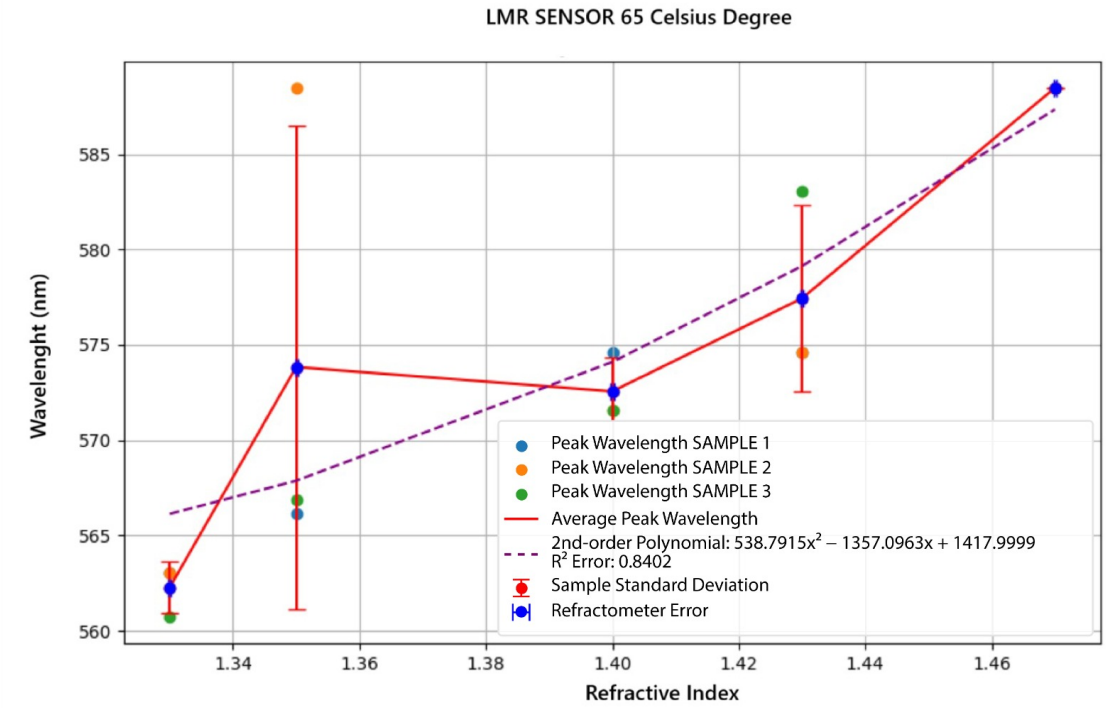

Source: Own authorship

Figura 21 – LMR Calibration Report at Temperature 65°C

RI	1.33	1.35	1.40	1.43	1.47
PICO wavelength [nm] - No treatment	563,04	566,13	574,61	574,61	588,47
PICO wavelength [nm] - No treatment	563,04	588,47	571,53	574,61	588,47
PICO wavelength [nm] - No treatment	560,73	566,90	571,53	583,08	588,47
PICO wavelength [nm] - No treatment - AVERAGE	562,27	573,83	572,56	577,43	588,47
SAMPLE STANDARD DEVIATION	1,33	12,68	1,78	4,89	0,00

```
Second-order polynomial: 538.7915x²-1357.0963x+1417.9999
R² error: 0.8402
Refractometer error: ±0.0002
Using the peak detection method: No treatment
```

Source: Own authorship

LMR Sensor 65 °C

$$\text{Sensitivity} = \frac{588{,}47\,\text{nm} - 562{,}27\,\text{nm}}{1{,}474 - 1{,}333} = \frac{24{,}14\,\text{nm}}{0{,}14} = 187{,}14\,\text{nm/RIU} \tag{10}$$

which in practice means that for each variation of 1 refractive index unit (1 RIU), the sensor's resonance peak shifts 187.14 nanometers in the spectrum. Figure 21 shows the calibration report generated by Python code.

In this case, the sensitivity of the sensor varied with each thermal cycle. At room temperature, the sensor showed the highest sensitivity value, at 65 °C sensibility fell into 54,14% of the value at room temperature. Therefore, we must consider temperature as a critical factor in the measurements taken. The increase in temperature can impact the evanescent field of LMRS sensors in several ways, mainly due to changes in the optical properties of the materials involved. In fiber optic-based sensors, temperature can affect the absorption of the evanescent wave, thereby altering the sensor's sensitivity. In addition, thermal variations can modify the mobility of charge carriers in semiconductors, influencing the sensor's response (Del Villar et al., 2025).

5.2 RESULTS AND INTEGRATED ANALYSIS OF INSULATING OIL TESTS

5.2.1 Experimental Methodology

The tests were performed on four samples of insulating oil, designated A, B, C, and D, to analyze the variation in refractive index when subjected to different thermal conditions and correlating this behavior with the physical and chemical properties of each sample. The measurements were performed using an LMR sensor coupled to a Peltier cell for precise thermal control, with the aid of an FBG sensor for temperature monitoring. The applied temperature range varied from 25°C to 60°C. These conditions are close to the operating range of three-phase transformers (55°C). For each sample, three complete thermal cycles were performed, evaluating the optical response of the system based on the spectral shift measured by the sensor.

Data:

- Sample A;
- RI=1,48;
- $\Delta\ \lambda$ in Thermal Cycles = 17.36 nm - Shift to blue wavelength.

Figura 22 – Sample A - Data 25°C to 60°C - Thermal Cycles

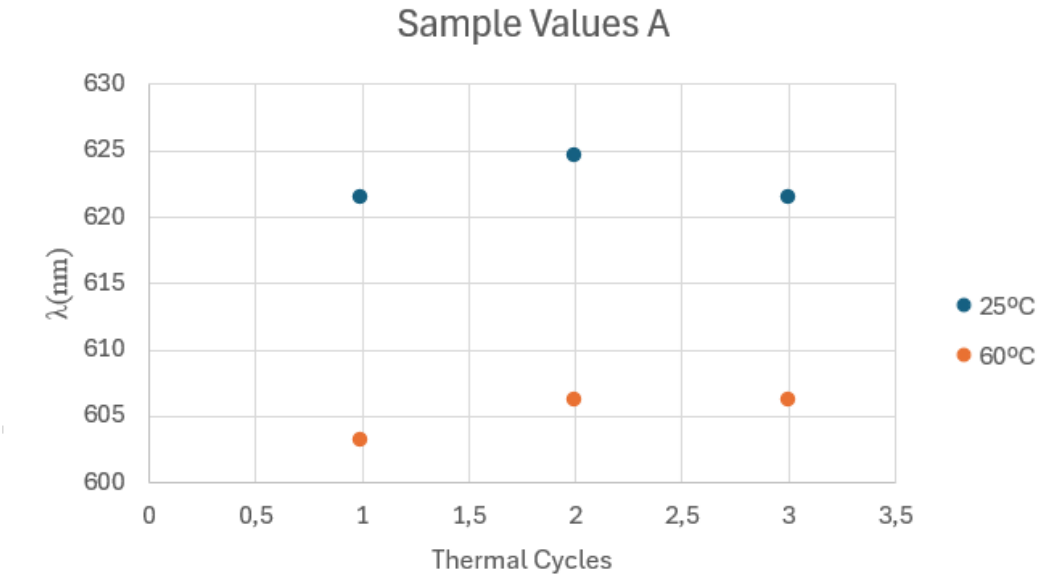

Sample A		25°C	60°C
Cycle 1	λ (nm)	621,49	603,15
Cycle 2	λ (nm)	624,55	606,15
Cycle 3	λ (nm)	621,49	606,15

Source: Own Authorship

In tests conducted with sample A, when varying the temperature from 25°C to 60°C, the espectral shift is 17.36 nm. This proves that the sample responded as expected when subjected to an increase in temperature. This behavior occurs in most liquids: as the temperature rises, the refractive index falls. It is an almost linear relationship in many oils and is used, for example, in refractometers with temperature compensation (see Figure 22).

- Sample B;
- RI=1,46;
- $\Delta\ \lambda$ in Thermal Cycles = 5.37 nm - Shift to blue wavelength.

Figura 23 – Sample B - Data 25°C to 60°C - Thermal Cycles

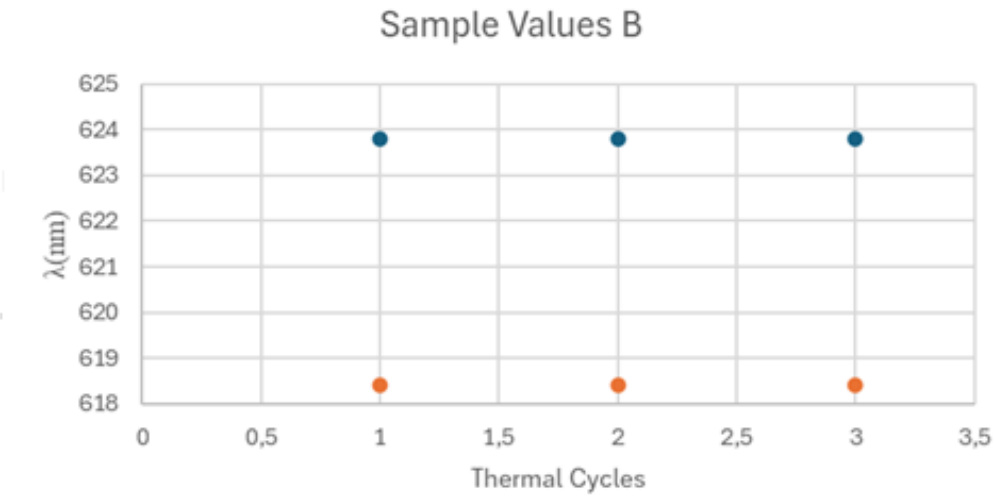

Sample B		25°C	60°C
Cycle 1	λ (nm)	623,79	618,42
Cycle 2	λ (nm)	623,79	618,42
Cycle 3	λ (nm)	623,79	618,42

Source: Own Authorship

In tests conducted with sample B, when varying the temperature from 25°C to 60°C, the spectral shift is 5,37 nm.A spectral shift much less pronounced than in the sample with newer oil (See Figure 23).

- Sample C;
- RI=1,46;
- $\Delta\ \lambda$ in Thermal Cycles = 33,59 nm - Shift to blue wavelength.

Figura 24 – Sample C - Data 25°C to 60°C - Thermal Cycles

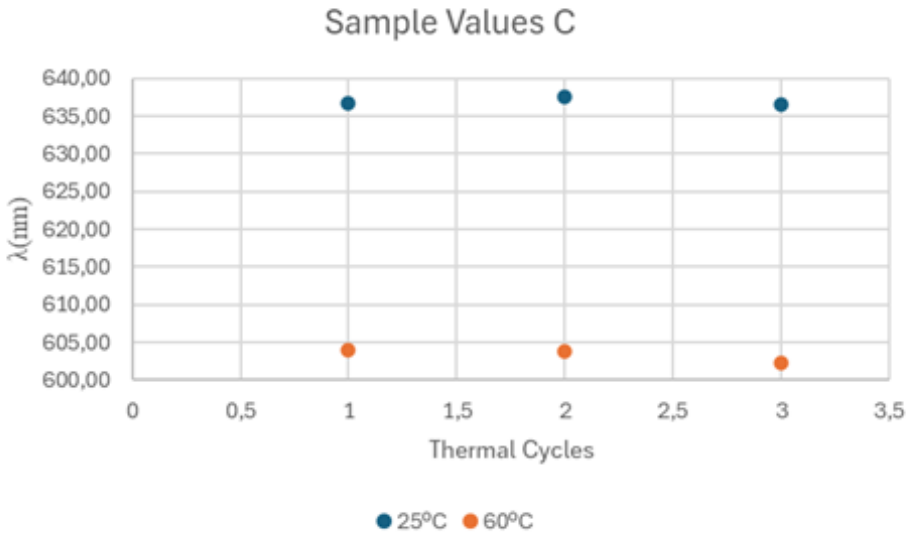

Sample C		25°C	60°C
Cycle 1	λ (nm)	636,80	604,01
Cycle 2	λ (nm)	637,57	603,84
Cycle 3	λ (nm)	636,57	602,31

Source: Own Autorship

In tests performed with sample C, when varying the temperature from 25 °C to 60 °C, the spectral change is 33.60 nm. This proves that the sample also responded as expected when subjected to an increase in temperature, a behavior similar to that of sample A. This behavior occurs in most liquids: as the temperature increases, the refractive index decreases. It is an almost linear relationship in many oils and is used, for example, in temperature-compensated refractometers (see Figure 24).

- Sample D;
- RI=1,48;
- $\Delta\ \lambda$ in Thermal Cycles = 4.82 nm - Shift to blue wavelength.

Figura 25 – Sample D - Dados 25°C to 60°C - Thermal Cycles

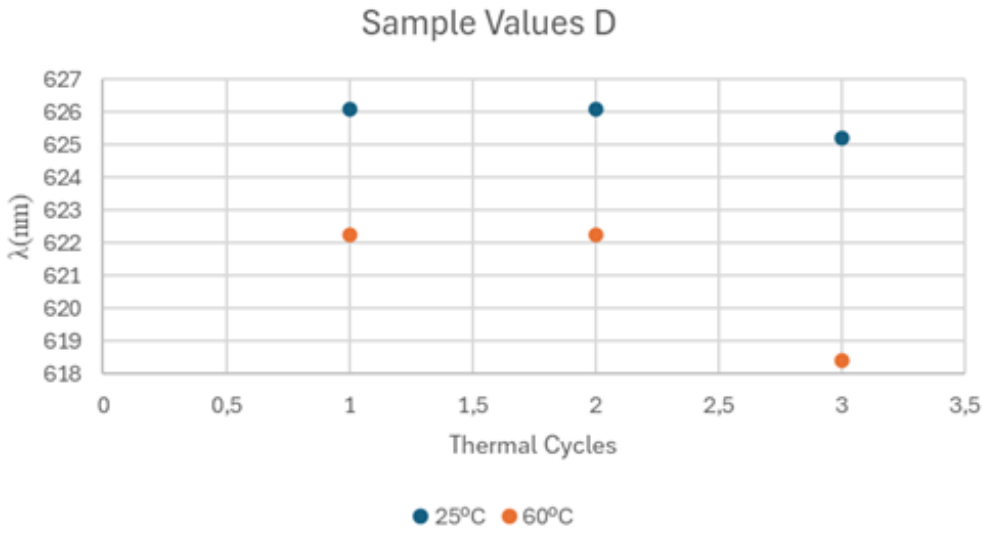

Sample D		25°C	60°C
Cycle 1	λ (nm)	626,09	622,26
Cycle 2	λ (nm)	626,09	622,26
Cycle 3	λ (nm)	625,22	618,42

Source: Own Autorship

In tests conducted with sample B, when varying the temperature from 25°C to 60°C, the spectral shift is 4,34 nm. A spectral shift much less pronounced than in the sample with newer oil (See Figure 25).

The samples with the greatest spectral shift ($\Delta\lambda$) are those with fewer hours of operation or samples of new oil (Sample A and Sample C). On the other hand, samples with oil that has a higher number of operating hours and is semi-degraded (Samples B and C) showed lower spectral shift ($\Delta\lambda$). These results will be discussed in detail in section 6.2.

5.3 INTEGRATED DISCUSSION OF RESULTS

The purpose of this chapter is to conduct a critical and integrated analysis of the results obtained throughout this research. Unlike the isolated presentation of findings, here we seek to compare and articulate the data with the theoretical references previously discussed in chapters 2 and 3. This approach allows for a more comprehensive understanding of the implications of the results, highlighting both their convergences and possible divergences in relation to previous works. Based on the sources provided, a summary of the conditions of each sample of insulating oil analyzed is presented, as well as the respective reports (diagnoses) issued by the certifying company in accordance with the criteria adopted by it.

5.3.1 Summary of Conditions and Sample Reports

The Insulating Oil Test Reports issued by the certified company detail the physical, chemical, and chromatographic conditions of transformer oil. Each report includes information about the customer and the equipment from which the sample was collected, such as power and voltage class, and compares the analysis results with the reference values established by technical standards, such as NBR-7070. The diagnoses generally indicate normal operating conditions and recommend a new analysis in 12 months, although one specific report (Sample D) indicates that the dielectric strength and water content are outside the limits and suggests oil treatment. In the report on the new oil sample (Sample C), we note that gas chromatography analysis was not performed. All reports were signed by a certified laboratory.

Tabela 2 – Summary of Sample A (Nº 382787, Romagnole) – Analysis on August 15, 2024

Parameter/Condition	**Result**
Operational Condition	OPERACIONAL
Equipment Power	1500 kVA
Dielectric Strength(Mín. Ref. 40,0 kV)	68,0 kV
Water Content (Máx. Ref. 40,0 ppm)	1,0 ppm
Visual Appearance	Clear
Neutralization Index	0,02 mg KOH/g
Report: Indication of normal operating conditions. A new analysis is recommended in 12 months and replacement of saturated silica gel.	

Tabela 3 – Summary of Sample B (Masterboi) – Analysis on September 8, 2024

Parameter/Condition	**Result**
Operational Condition	OPERACIONAL
Equipment Power	1000 kVA
Dielectric Strength (Mín. Ref. 40,0 kV)	68,0 kV
Water Content (Máx. Ref. 40,0 ppm)	1,0 ppm
Visual Appearance	Clear
Neutralization Index	0,01 mg KOH/g
Report: Normal operating conditions, according to Filtroil criteria. A new analysis is recommended in 12 months and replacement of saturated silica gel.	

Tabela 4 – Summary of Sample C – New Oil (UTFPR) – Analysis on October 12, 2024

Parameter/Condition	**Result**
Oil Type	New Transformer Oil
Client	UTFPR
Dielectric Strength (Mín. Ref. 40,0 kV)	75,0 kV
Water Content (Máx. Ref. 40,0 ppm)	0,5 ppm
Visual Appearance	Clear
Neutralization Index	0,01 mg KOH/g
Gas Chromatography Analysis	Unrealized
Report: Normal operating conditions. It is recommended that a new analysis be performed in 12 months and that the saturated silica gel be replaced.	

Tabela 5 – Summary of Sample D (Nº 404278, União) – Analysis on September 5, 2024

Parameter/Condition	Result
Operational Condition	FILTERING
Manufacturer / Year	União / 1988
Dielectric Strength (Mín. Ref. 40,0 kV)	35,6 kV (Out of bounds)
Water Content (Máx. Ref. 40,0 ppm)	22 ppm
Visual Appearance	Clear
Neutralization Index	0,01 mg KOH/g

Report: Dielectric strength and water content outside limits. Treatment of oil with a thermal vacuum filter is recommended.
Note: There is a secondary report indicating normal operating conditions, suggesting a new analysis in 12 months. However, the specific diagnosis shows flaws in rigidity and water content. Replacement of saturated silica gel is also recommended.

5.4 CORRELATION BETWEEN SPECTRAL SHIFT AND PHYSICAL-CHEMICAL ANALYSIS

In the LMR sensor tests, samples B and D showed the lowest spectral shift. This behavior may be directly related to high CO_2 levels, indicating possible oil degradation, even though sample B was considered operational in the physical-chemical tests. This finding suggests that, although in acceptable operational condition, sample B may be in the early stages of degradation, as revealed by the spectral response to temperature variation. This correlation reinforces the importance of complementary analyses, in addition to routine ones, for a more robust predictive assessment of the condition of insulating oil.

Tabela 6 – Results of Tests with Temperature Variation in Insulating Oil

Sample	Refractive Index	$\Delta\ \lambda$ (nm)	Δ(n)
A	1,48	17,36	-0,05
B	1,46	5,37	-0,01
C	1,46	33,60	-0,10
D	1,48	4,34	-0,01

max width=

5.5 HIGHLY CORRELATED PHYSICAL-CHEMICAL PARAMETERS - SAMPLES B AND D

Both samples had a **neutralization index (acidity)** of 0.01 mg KOH/g, an extremely low value and well below the maximum reference limit of 0.20 mg KOH/g, indicating reduced acid degradation of the oil. The **visual appearance** was clear in both samples. As for the **water content**, although Sample D showed dielectric strength outside the limit, the water content remained within the reference range of 40 ppm, being 1.0 ppm for Sample B and 22 ppm for Sample D. Maintenance recommendations indicate the replacement of saturated silica gel in both samples. The analyses were performed in September 2024, with a time difference of only three days between them.

5.6 CORRELATION IN DISSOLVED GASES (DGA)

- **Carbon Dioxide (CO_2)**: Both showed extremely high levels, well above the limit of 20,000 ppm (Sample B: 45842 ppm and Sample D: 54907 ppm)

  This parameter suggests degradation of the solid insulating paper, even though the neutralization index is low.

- **Hydrogen (H_2)**: Absent in both analyses (0 ppm).

5.7 KEY DIFFERENCES

Despite the similarities, the samples have different operating conditions:

Tabela 7 – Comparison between Samples B and D

max width=

Parameter	**Sample B (OPERACIONAL)**	**Sample D (FILTERING)**
Dielectric Strength (Mín. 40,0 kV)	68,0 kV (Excellent)	35,6 kV (Out of bounds)
Methane (CH_4) (Máx. 500 ppm)	1521 ppm (Over the limit)	7 ppm (Within the limit)
Diagnosis	Operacional	Not Operational*

* Dielectric strength and water content (Out of range)- Sample D

5.8 INFLUENCE OF CHEMICAL COMPOSITION ON OPTICAL RESPONSE - ALL SAMPLES

The results show that wavelength variation is strongly related to the physical and chemical properties of the samples:

- **Water Content (H_2O):** The presence of water, a highly polar substance, significantly influences the refractive index.

  The samples with lower water content (A: 8 ppm; C: 12 ppm) showed greater spectral shifts (17.36 nm and 33.6 nm, respectively), while the samples with higher water content (B: 16 ppm; D: 16 ppm) exhibited less spectral variation (5.37 nm and 4.34 nm). The increase in water favors the formation of micelles and emulsions, altering the optical structure of the oil.(INSTITUTE OF ELECTRICAL AND ELECTRONICS ENGINEERS (IEEE), 2013)

- **Concentration of combustible gases** High levels of gases, as in the sample **D** (216 ppm), indicate **advanced degradation** of the oil, compromising dielectric uniformity and reducing optical variation.

- **Dielectric strength:** Samples **A**, **B**, and **C** showed acceptable values (75,0 kV/2.5 mm), while sample **D** showed significantly lower rigidity (35,6 kV/2.5 mm), showing signs of aging.

5.9 EFFECT OF TEMPERATURE ON REFRACTIVE INDEX

With the increase in temperature, a spectral shift toward blue was observed in all samples, indicating a **reduction in the refractive index**. This occurs due to the decrease in oil density and the partial volatilization of the water present.

The relationship between density, molecular polarizability, and refractive index is described by the Lorentz–Lorenz equation, already explored in Chapter 2 - Fundamentals of Refractive Index.

5.10 GENERAL CORRELATION BETWEEN DEGRADATION AND OPTICAL

RESPONSE

- New or slightly degraded samples (**C** and **A**) exhibited greater optical sensitivity, showing significant shifts in wavelength.
- **More degraded** samples (**D** and, to a lesser extent, **B**) showed **low spectral variation**, correlating with higher water content, high presence of combustible gases, and reduced dielectric strength.

This correlation confirms the effectiveness of the LMR sensor in detecting physical and chemical changes associated with the degradation of insulating oil.

6 CONCLUSION

The degradation of insulating oil in transformers can lead to critical operational failures, compromising their functionality due to the loss of insulating properties. Throughout their service life, transformer windings and insulation face significant mechanical, thermal, and chemical stresses. Water dissolved in oil accelerates insulation degradation, reduces dielectric strength, and decreases the maximum voltage that the oil can withstand without suffering damage. Traditional methods of analyzing insulating oil content are costly and require specialized laboratory infrastructure. This study analyzed four samples of insulating oil from transformers in operation (A, B, C, and D) under different operating conditions and states of degradation. A fiber optic sensor based on loss mode resonance (LMR) with ZnO coating was used. The experimental setup included an AQ 4305 (Yokogawa) white light source with a wavelength range of 400–1600 nm and an Ocean Optics QE65000 spectrometer, which measures between 200–1100 nm. The LMR sensor was calibrated to achieve a sensitivity of 345.78 nm/RIU. The sensor's response to the four oil samples (A, B, C, and D) was evaluated in three thermal cycles, with temperatures ranging from 25 °C to 60 °C, in accordance with IEC 60076-3.

- The **LMR** sensor demonstrated **high sensitivity** to variations in refractive index, allowing optical changes to be correlated with the **physical-chemical parameters** of the samples. Thus, any change in the physical-chemical composition of the medium (in this case, the insulating oil) that results in a variation, even if very small, in the refractive index of the samples, modulated the coupling conditions, causing a detectable shift in the resonance wavelength, noticeable in the results graphs, as demonstrated in Chapter 5.

- The **presence of water** and **combustible gases** was decisive in reducing spectral displacement, reflecting the **operational degradation** of the oils. The increase in water favors the formation of micelles and emulsions within the oil, which alters the optical structure of the medium. This compromises the optical uniformity and IR capacity of pure oil to respond linearly to temperature, reducing the detectable optical variation. The presence of water also accelerates insulation degradation and reduces the dielectric strength of the oil over the operating time of the transformer.

- Traditional insulating oil monitoring—which includes tests for Dielectric Breakdown Voltage (DBV), Acidity, Power Factor, Water Content, and Dissolved Gas Analysis (DGA)—is essential to ensure reliability and extend the service life of transformers. However, these methods have limitations. Optical monitoring can be used as a complementary method to traditional physical-chemical analyses, providing rapid and

non-destructive diagnostics on the health of insulating oil.

The study corroborated the effectiveness of the LMR sensor in identifying stages of degradation that are often overlooked by conventional routine analyses. The device demonstrated the ability to detect critical risk factors, such as the presence of water and combustible gases, whose influence was decisive in reducing spectral displacement. It was found that higher levels of these elements, traditionally associated with advanced degradation processes and loss of dielectric uniformity, correlated with reduced spectral variations.

In addition, the LMR showed significant performance in early fault detection. In the case of Sample B, for example, although classified as "OPERATIONAL" according to the physical-chemical report, a significantly lower spectral shift was observed during thermal cycles (5.37 nm) compared to new samples (A and C). This result suggests that the optical sensor is sensitive enough to reveal early stages of degradation that are not captured by traditional routine tests. Thus, it can be concluded that optical monitoring is a robust, agile, and operationally simplified predictive diagnostic tool that overcomes the limitations inherent in conventional methods. In addition to enabling the identification of physical-chemical changes in a short time, this approach minimizes the need for complex and costly laboratory analyses, presenting itself as an efficient alternative for monitoring the performance and integrity of dielectric systems.

In summary, LMR technology represents a flexible and versatile approach to optical sensing, leveraging the interaction of the fiber's evanescent wave with specific thin films to detect environmental changes with high sensitivity. This technology has not yet been fully explored with all gas-sensitive materials, indicating great potential for research. Trends include increasing sensitivity by combining different materials and complex geometric shapes, using special or microstructured fibers (D-type, hollow, photonic crystal) for sharper resonance peaks and larger surface area. There is also a trend toward reducing costs by using substrates such as glass coverslips to enable large-scale use in areas such as smart cities.

REFERENCES

ABNT. **Transformadores de Potência: Parte 5 – Capacidade de Resistir a Curtos-Circuitos**. Rio de Janeiro, RJ, dez 2007. 18 p.

ABNT. **Transformadores de Potência: Interpretação da análise dos gases de transformadores em serviço**. Rio de Janeiro, RJ, dez 2012. 18 p.

AGRAWAL, G. P. **Fiber-Optic Communication Systems**. 4th. ed. Wiley, 2012.

Agência Nacional de Energia Elétrica. **National Agency of Electric Energy**. 6 2024. 01-05 p. Disponível em: https://www.gov.br/aneel/pt-br/assuntos/noticias/2024.

AL-FAKIH, E.; OSMAN, N. A. A.; ABAS, W. A. B. W. The use of fiber bragg grating sensors in biomechanics and rehabilitation applications: The state-of-the-art and ongoing research topics. **Sensors**, MDPI, v. 12, n. 10, p. 12890–12926, 2012. ISSN 1424-8220. Review article discussing the use of Fiber Bragg Grating (FBG) sensors in biomechanics and rehabilitation engineering. Disponível em: https://www.mdpi.com/1424-8220/12/10/12890.

ASSIS, M.; CAMARGO, M. **Código Python LMR - Software Colaborativo**. UTFPR, 2024.

AZIS, N.; ZHOU, D.; WANG, Z. D.; JONES, D.; WELLS, B.; WALLWORK, G. Operational condition assessment of in-service distribution transformers. In: **2012 IEEE International Conference on Condition Monitoring and Diagnosis**. 2012. p. 1156–1159.

CHIAVAIOLI, F.; JANNER, D. Fiber optic sensing with lossy mode resonances: Applications and perspectives. **J. Lightwave Technol.**, Optica Publishing Group, v. 39, n. 12, p. 3855–3870, Jun 2021. Disponível em: https://opg.optica.org/jlt/abstract.cfm?URI=jlt-39-12-3855.

CIGRÉ Working Group A2. **Technical Brochures on Transformer Condition Assessment and Monitoring**. Paris, France, 2015. Publicações técnicas do CIGRÉ sobre avaliação e monitoramento de transformadores.

CORREA-FERNáNDEZ, A.; GALLEGO-MARTíNEZ, E. E.; RUIZ-ZAMARREñO, C.; MATíAS, I. R. Lossy mode resonance and hyperbolic mode resonance-based optical sensors by means of y3fe5o12 and srtio3 films deposition on planar substrates. **IEEE Sensors Letters (Implicação do DOI e Contexto)**, Não Especificado, p. Não Especificado, jul 2025. Manuscrito recebido 30 de abril de 2025; Revisado 11 de junho de 2025; Aceito 29 de junho de 2025; Data de publicação 2 de julho de 2025 [1].

Del Villar, I.; IMAS, J. J.; MATIAS, I. R. A review on lossy mode resonance-based sensors: Fundamentals and applications. **Sensors and Actuators B: Chemical**, v. 444, p. 138421, 2025. ISSN 0925-4005. Disponível em: https://www.sciencedirect.com/science/article/pii/S0925400525011979.

FIGUEIREDO, M. V. A. F. d.; MARTINS-FILHO, J. F. Detecção Óptica no infravermelho de furano em amostras de Óleo isolante de transformador. In: **Anais do Grupo de Fotônica, Departamento de Eletrônica e Sistemas, Universidade Federal de Pernambuco**. Recife-PE, Brasil, 2005. Fone: (81) 2126-7784, e-mail: jfmf@ufpe.br.

FILHO, M. J.; NONATO, G. A.; MIYAMOTO, E. T.; SCUCUGLIA, J. W.; CRUZ, L. C.; JÚNIOR, A.; REIS, M.; SUZUQUI, M.; FARIA, U. C. Desenvolvimento de sensor infravermelho para detecção on-line de gases dissolvidos em óleo isolante de transformadores.

FRIEDENBERG, L. E.; SANTANA, R. M. C. Propriedades de óleos isolantes de transformadores e a proteção do meio ambiente. **LX Simpósio Internacional De Qualidade Ambiental. Porto Alegre-RS. Energia e Ambiente**, p. 1–12, 2014.

GUO, C.; DONG. A review of on-line condition monitoring in power system. In: **2019 IEEE 8th International Conference on Advanced Power System Automation and Protection (APAP)**. 2019. p. 634–637.

IEC 60599. **IEC 60599: Mineral oil-filled electrical equipment in service – Guidance on the interpretation of dissolved and free gases analysis**. 2015. 3rd edition.

IMAS, J.; VILLAR, I. D.; ZAMARREñO, C. R.; MATíAS, I. R. Optical fiber sensors based on lossy mode resonances (lmrs): Fundamentals and recent developments. In: **2023 23rd International Conference on Transparent Optical Networks (ICTON)**. 2023. p. 1–4.

INSTITUTE OF ELECTRICAL AND ELECTRONICS ENGINEERS (IEEE). **IEEE Guide for Diagnostic Field Testing of Fluid-Filled Power Transformers, Regulators, and Reactors**. New York, USA, 2013. Guia IEEE para ensaios de diagnóstico em transformadores de potência imersos em óleo.

ISLAM LEE, G.; HETTIWATTE, S. A review of condition monitoring techniques and diagnostic tests for lifetime estimation of power transformers. **Electr Eng 100**, p. 581–605, 2018.

JIN, L.; KIM, D.; ABU-SIADA, A.; KUMAR, S. Oil-immersed power transformer condition monitoring methodologies: A review. **Energies**, MDPI, v. 15, n. 9, p. 3379, 2022.

KO, J. H.; YOO, Y. J.; LEE, Y.; JEONG, H.-H.; SONG, Y. M. A review of tunable photonics: Optically active materials and applications from visible to terahertz. **IScience**, Elsevier, v. 25, n. 8, 2022.

KUZNETSOV, P.; SUDAS, D.; SAVELYEV, E. Fiber optic lossy mode resonance based sensor for aggressive liquids. **Sensors and Actuators A: Physical**, Elsevier, v. 321, p. 112576, 2021.

LIU, D. M. **Electromagnetic and Photonic Simulation for the Beginner: Finite-Difference Frequency-Domain in MATLAB®**. Norwood, MA: Artech House, 2018. (Artech House Applied Photonics Series).

LU, P.; BURIC, M. P.; BYERLY, K.; MOON, S. R.; NAZMUNNAHAR, M.; SIMIZU, S.; LEARY, A. M.; BEDDINGFIELD, R. B.; SUN, C.; ZANDHUIS, P.; MCHENRY, M. E.; OHODNICKI, P. R. Real-time monitoring of temperature rises of energized transformer cores with distributed optical fiber sensors. **IEEE Transactions on Power Delivery**, v. 34, n. 4, p. 1588–1598, 2019.

MANUAL, O. Installation and operation manual. **gas**, v. 4, n. Y3, p. Y2, 2015.

MATTEDE, H. **O que são linhas de transmissão Características e Curiosidades**. 2025.

MEITEI, S. N.; BORAH, S. Review on monitoring of transformer insulation oil using optical fiber sensors. **Results in Optics**, Elsevier, v. 10, p. 100361, 2023.

PALIWAL, N.; JOHN, J. Lossy mode resonance (lmr) based fiber optic sensors: A review. **IEEE Sensors Journal**, IEEE, v. 15, n. 10, p. 5361–5371, 2015.

PAVIA, D. L.; LAMPMAN, G. M.; KRIZ, G. S.; VYVYAN, J. R. **Introdução à espectroscopia**. Cengage Learning, 2010.

PORTO EDITORA. **Permitividade – no Dicionário infopédia da Língua Portuguesa**. Porto Editora, 2025. [Acesso em: 07 out. 2025, 20:16:53]. Disponível em: https://www.infopedia.pt/dicionarios/lingua-portuguesa/permitividade.

POSSETTI, G. R. C. **Sensores em fibra ótica para avaliação de combustíveis líquidos**. 2013. 183 p. Tese (Tese de Doutorado) — Universidade Tecnológica Federal do Paraná (UTFPR), Curitiba, 2013. Programa de Pós-Graduação em Engenharia Elétrica e Informática Industrial; Área de Concentração: Fotônica em Engenharia; Coorientadora: Marcia Muller.

SALEH, B. E. A.; TEICH, M. C. **Fundamentals of Photonics**. 2nd. ed. Hoboken, NJ: Wiley-Interscience, 2007. Descreve as propriedades de ondas evanescentes e os princípios de acoplamento modal, sendo uma excelente fonte para o estudo de acoplamento entre modos e perda de energia em filmes finos. ISBN 978-0-471-35832-9.

SPACCKOVA, B.; JR, N. S. L.; SLABYYY, H.; HOMOLA. A route to superior performance of a nanoplasmonic biosensor: consideration of both photonic and mass transport aspects. **Acs Photonics**, ACS Publications, v. 5, n. 3, p. 1019–1025, 2018.

TROPF, W. J.; THOMAS, M. E.; LINEVSKY, M. J. Infrared refractive indices and thermo-optic coefficients for several materials. In: SPIE. **Optical Diagnostic Methods for Inorganic Transmissive Materials**. 1998. v. 3425, p. 160–171.

VILLAR, I. D.; ARREGUI, F. J.; ZAMARREÑO, C. R.; CORRES, J. M.; BARIAIN, C.; GOICOECHEA, J.; ELOSUA, C.; HERNAEZ, M.; RIVERO, P. J.; SOCORRO, A. B. et al. Optical sensors based on lossy-mode resonances. **Sensors and Actuators B: Chemical**, Elsevier, v. 240, p. 174–185, 2017.

VITORIA, I.; GALLEGO, E. E.; MELENDI-ESPINA, S.; HERNAEZ, M.; ZAMARREÑO, C. R.; MATÍAS, I. R. Gas sensor based on lossy mode resonances by means of thin graphene oxide films fabricated onto planar coverslips. **Sensors**, MDPI, v. 23, n. 3, p. 1459, 2023.

WANG, J.; LI, Z.; FU, X.; GUI, X.; ZHAN, J.; WANG, H.; JIANG, D. High-sensing-resolution distributed hot spot detection system implemented by a relaxed pulsewidth. **Optics Express**, Optica Publishing Group, Washington, DC, v. 28, n. 11, p. 16045–16055, 2020. Research Article, published 25 May 2020. Disponível em: https://opg.optica.org/oe/fulltext.cfm?uri=oe-28-11-16045.

ZUBIATE, P.; CORRES, J. M.; ZAMARREÑO, C. R.; MATIAS, I. R.; ARREGUI, F. J. Fabrication of optical fiber sensors for measuring ageing transformer oil in wavelength. **IEEE Sensors Journal**, IEEE, v. 16, n. 12, p. 4798–4802, 2016.

APPENDIX A – PHOTOS OF EXPERIMENTAL SETUPS

Photos of Experimental Setups and Equipment - Multi-user Laboratory - FOTON (UTFPR)

Experimental Calibration Bench – FOTON Laboratory

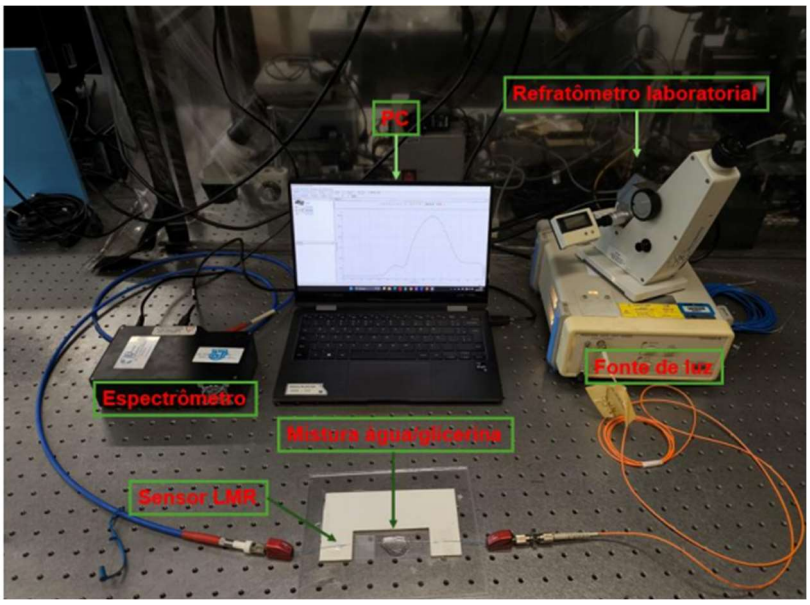

LMR Sensor Connection

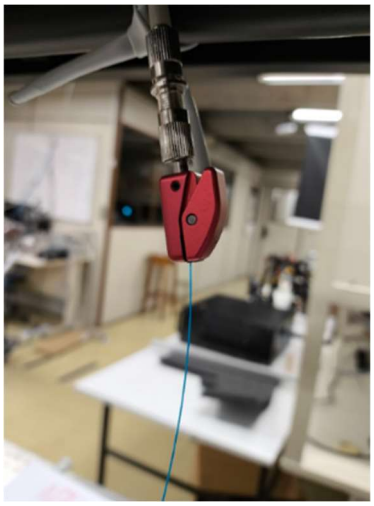

Sample A

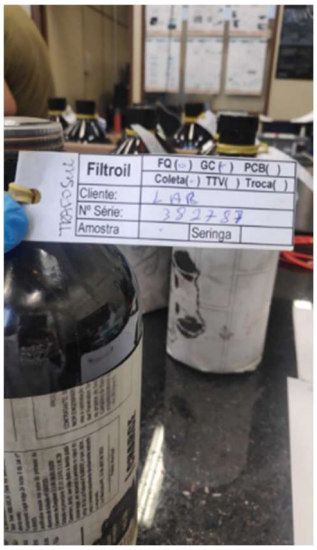

Sample B

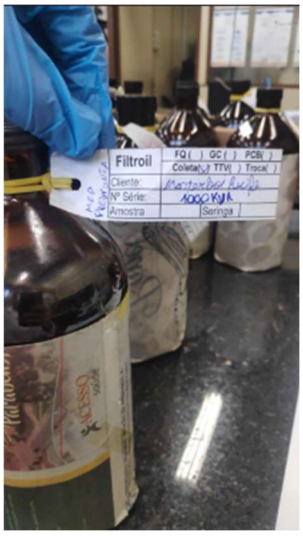

Temperature control with FBG

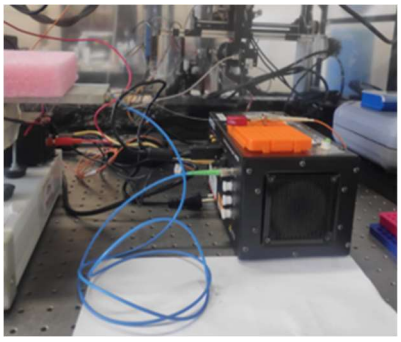

Setup with Temperature Control

Peltier Cell + Digital Controller

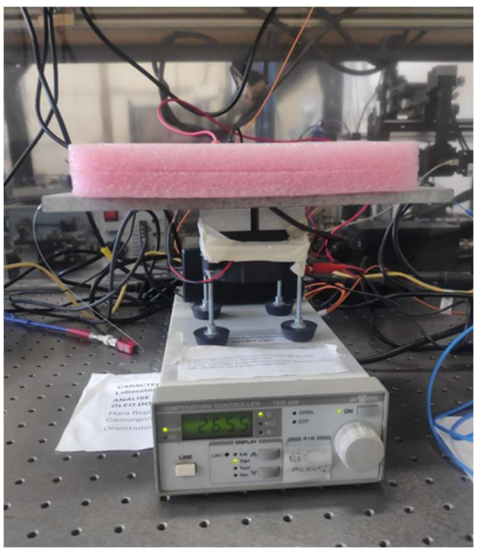

APPENDIX B – WORK CARRIED OUT AT THE PUBLIC UNIVERSITY OF NAVARRA

Introdution

After the ISOS 2025 Congress at the Public University of Navarra, the following two days were spent visiting the university's laboratories and, together with the UPNA research group, manufacturing some LMR sensors. The sensors manufactured were planar sensors which, in the context of studies conducted on LMRs, refers to the use of a planar waveguide configuration to support optical resonance phenomena, such as Loss Mode Resonance (LMR) and Hyperbolic Mode Resonance (HMR). This configuration has proven to be very successful in the field of optical sensors, as mentioned in studies by (VITORIA et al., 2023) and (CORREA-FERNáNDEZ et al., 2025).

The Manufacturing Process

More recently, Hyperbolic Mode Resonance (HMR) has been proposed as an optimized combination of LMR and Surface Plasmon Resonance (SPR). Both have demonstrated effectiveness in biomedical, environmental, and industrial applications. Many materials meet the refractive index requirements and can be used for their manufacture. Among the most frequently used are tin oxide(SnO_2),indium tin oxide (ITO), titanium dioxide (TiO_2) and certain groups of polymers. On this occasion, HMR sensors were manufactured with new materials in this field ($Y_3Fe_5O_{12}$) Yttrium iron garnet e ($SrTiO_3$) Strontium tritane. For HMR resonances, each sample was designed with a 25 nm thickness of intermediate gold thin film. Resonances were generated by RF sputtering of the aforementioned materials onto cover slips on a planar waveguide.

Sensors were also manufactured in (ZnO) Zinc Oxide e (Cuo_2)Copper Dioxide.

Figura 26 – Preliminary LMR Result on SubstrateZnO) Zinc Oxide with gold coating) - TE and TM

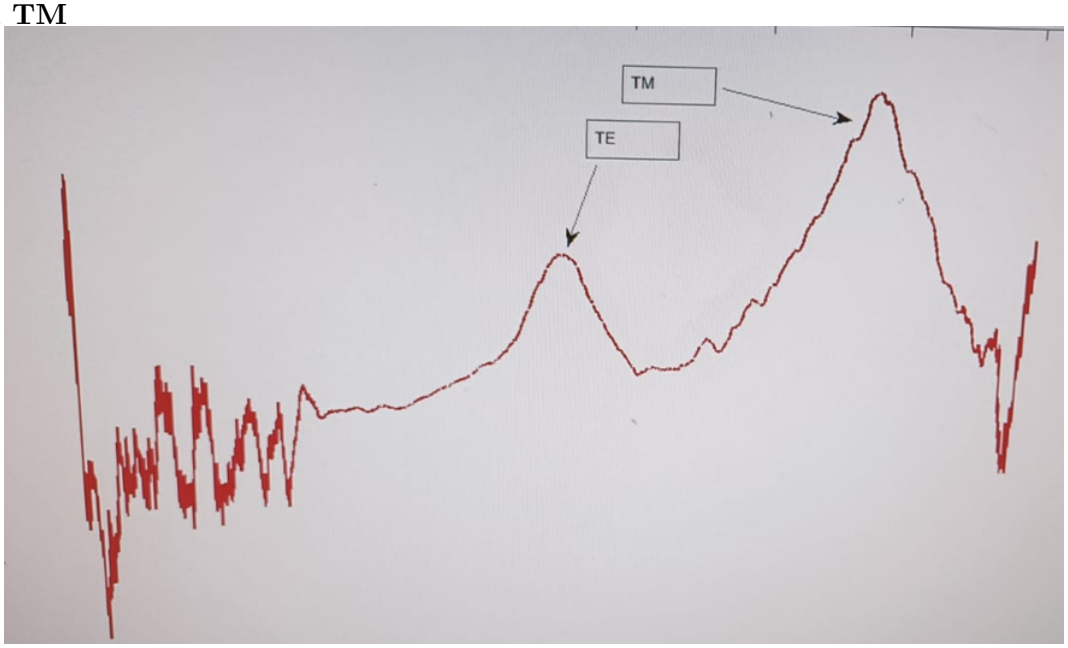

Source: Own Autorship

Figura 27 – Planar Sensor Manufacturing Process - RF

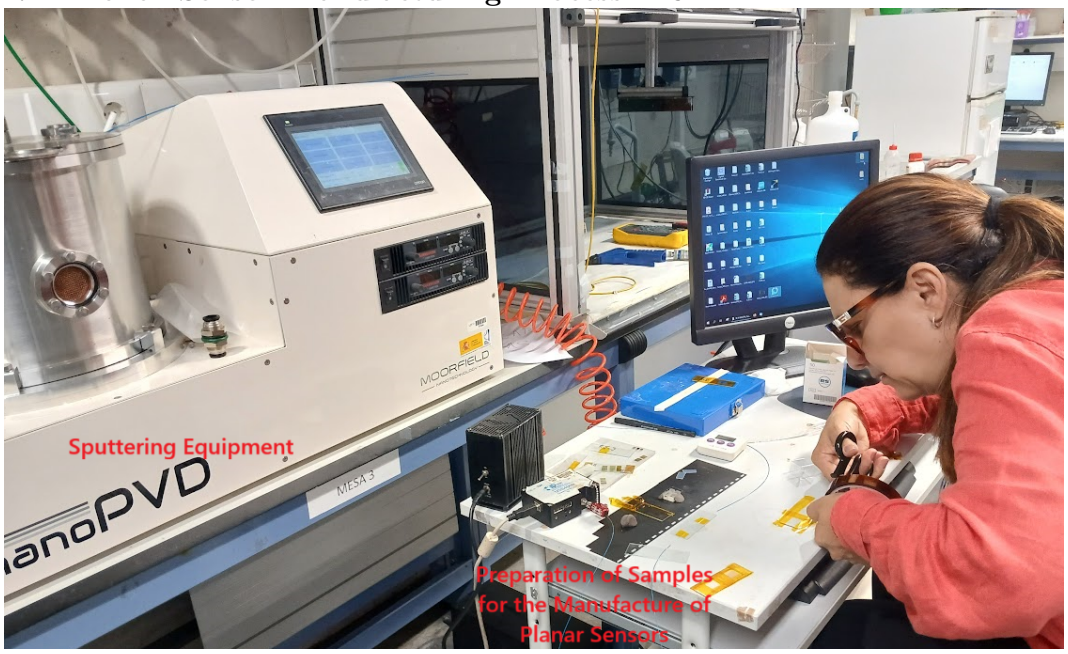

Source: Own Autorship

PVD Equipment Parameters – DC

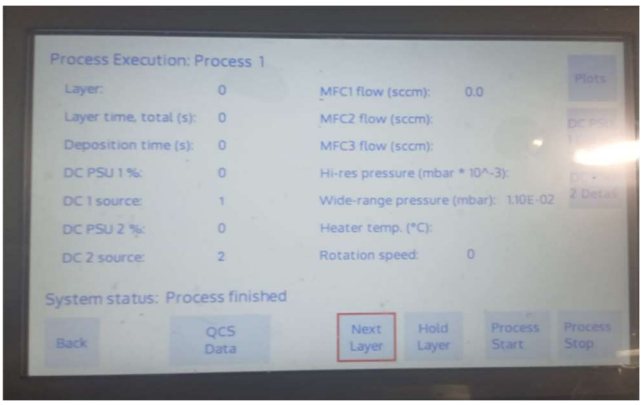

Air Sensor Spectrum

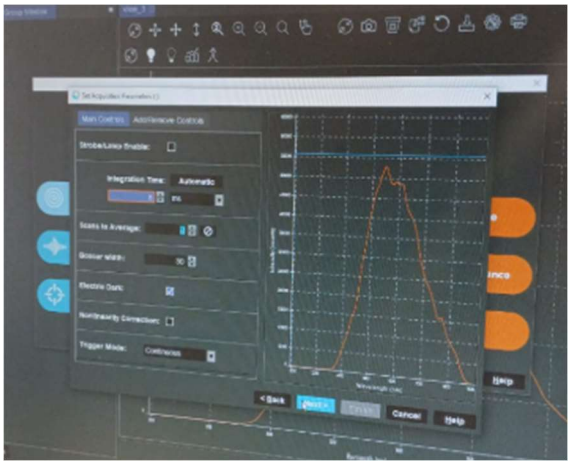

Sputtering Process

Planar Sensors

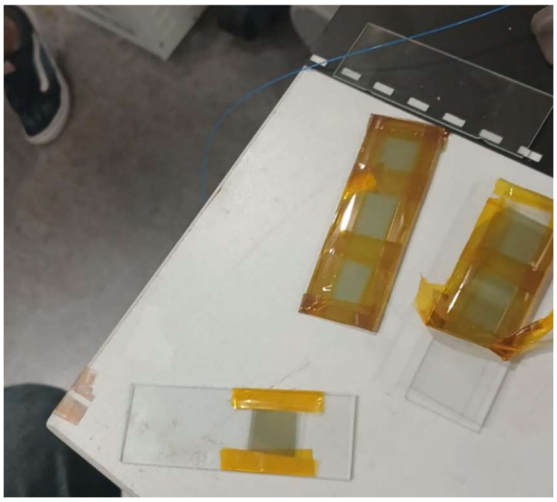

APPENDIX C – PARTICIPATION IN INTERNATIONAL CONFERENCE

Participation in the International Symposium on Optical Sensors (ISOS 2025), which promoted scientific exchange and fostered networking and collaborative ties among leading international researchers.

This thematic conference covers the frontiers of multidisciplinary research in engineering structure testing. The work presented in the Poster session was entitled: *ANALYSIS OF ELECTRIC TRANSFORMER INSULATION OIL USING LMR OPTICAL FIBER SENSOR*.

International Symposium on Optical Sensors
Pamplona, June 1st-3rd 2025

ANALYSIS OF ELECTRIC TRANSFORMER INSULATION OIL USING LMR OPTICAL FIBER SENSOR

Mara R. A. de Assis[1], Elaine Grabski[1], Matheus O. Camargo[1], Valmir Oliveira[1], Jean C. C. da Silva [1], Carlos R. Zamarreño[2], Pablo Zubiate[2], Uilian J. Dreyer[1]
[1] Federal University of Technology of Paraná, UTFPR – Brazil
[2]Electrical and Electronic Engineering Department, UPNA, Pamplona, Spain
Uilian José Dreyer (uiliandreyer@utfpr.edu.br)

ABSTRACT

Over its operational life, the transformer's windings and insulation face significant mechanical, thermal, and chemical stress that reduces dielectric strength and lowers the maximum voltage the oil can handle without damage [1]. This study examined insulating oil samples from operational transformers under varying functional conditions and degradation states, employing a fiber optic sensor based on lossy mode resonance (LMR) [2]. The experimental setup included a white light source AQ4305 (Yokogawa) and an Ocean Optics QE65000 spectrometer. The LMR sensor was calibrated using the experimental setup (Fig. 1(a)) to achieve a sensitivity of ~341 nm/RIU (Fig. 2.a). The sensor's response to two oil samples (A and B) was evaluated across three thermal cycles using the experimental setup presented in Fig. 1(b), with temperatures ranging from 25 °C to 60 °C. Figure 2 (b) shows the variation in wavelength in each of the three temperature cycles for the oil samples. Sample A exhibited a spectral blue shift of 17.4 nm (-0.05 RIU), while sample B showed a smaller shift of 5.4 nm (-0.01 RIU). The wavelength variation detected by the LMR sensor is attributed to the distinct physicochemical properties of each sample, as determined by a specialized laboratory (Table 1). Both samples presented a dielectric strength of 75.0 kV/2.5 mm, a value considered adequate according to operational parameters [3]. The greater shift in sample A may be related to its lower water content and higher total combustible gas levels. Sample B, with higher water content, showed a smaller RI shift (see equation (1)). Water, being highly polar, influences the refractive index and can promote the formation of micelles or emulsions, especially in degraded oils. With increasing temperature, it tends to dissolve or partially volatilize, forming bubbles or vapor, altering the medium's optical response.

ACKNOWLEDGEMENTS

The authors acknowledge to CNPQ, FINEP, Fundação Araucária, SETI and Multi-User Photonics Facility (UTFPR-CT). This study received partial financial support from CAPES - Finance Code 001.

REFERENCES

[1] L. De Maria, F. Scatiggio, M. Pesavento, N. Cennamo, and L. Zeni, "Toward an optical monitoring of chemical markers in transformers insulating oil," in 2019 IEEE 20th International Conference on Dielectric Liquids (ICDL), Jun. 2019, pp. 1–4. doi: 10.1109/ICDL.2019.8796737.

[2] I. Del Villar et al., "Design rules for lossy mode resonance-based sensors," Appl. Opt., vol. 51, no. 19, p. 4298, Jul. 2012, doi: 10.1364/AO.51.004298.

[3] BRAZILIAN ASSOCIATION OF TECHNICAL STANDARDS. ABNT NBR 10576:2017 – Mineral insulating oil for electrical equipment –Rio de Janeiro: ABNT, 2017.

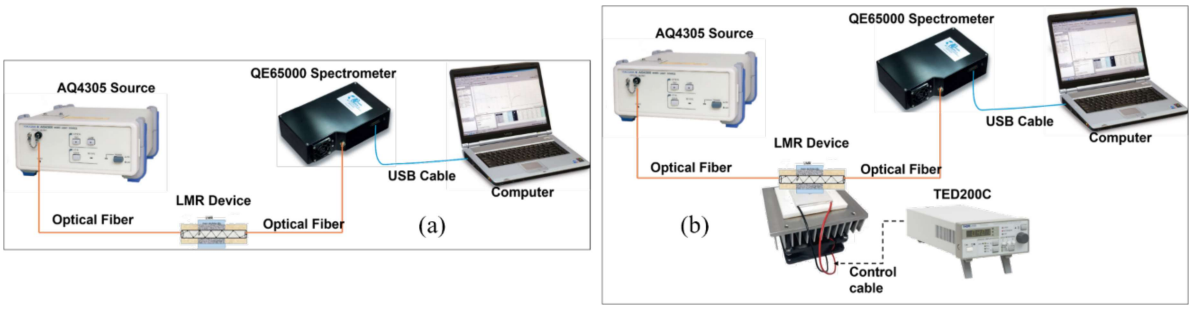

Figure 1. Experimental setup containing Light Source AQ4305 and a QE65000 Spectrometer; (a) for the calibration process; (b) for the insulation oil temperature testing

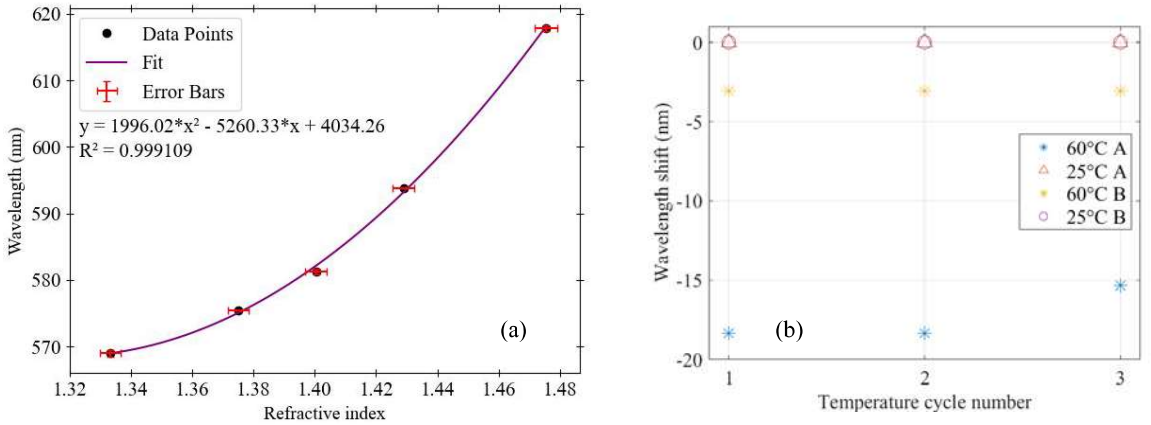

Figure 2. (a) LMR sensor calibration curve and second-degree polynomial fit. (b) LMR sensor wavelength shift results from the three heating cycles of samples A and B.

Table 1. Physicochemical oil samples properties.

Sample	**Refraction Index**	**Dielectric Strength** (kV/2.5 mm)	**Density 20/40°C** (g/cm³)	**Interfacial Tension** (dyne/cm)	**Water Content** (ppm)	**Combustible Gas** (ppm)
A	1.48 ⬆	75.0	0.892 ⬆	34.4	8.0	133 ⬆
B	1.46	75.0	0.837	39.5 ⬆	16.0 ⬆	21

*Notes: Sample A shows lower water content, higher gas concentration, and lower interfacial tension, suggesting impurities as the wavelength increases with heat. Sample B exhibits higher water content, higher interfacial tension, and typical behavior where oil's density and wavelength decrease with heat. The refractive index, influenced by medium density, is related to light's speed in different materials, as expressed by the Lorentz-Lorenz equation (1):

$$n^2 = 1 + {}^{4\pi N\alpha}/_{3}, \quad (1)$$